

# UC Davis

## UC Davis Electronic Theses and Dissertations

### Title

Closing the Loop: Integrating Control and Sensory Feedback for Individuals with Upper Limb Loss and N-TMR Surgery

### Permalink

<https://escholarship.org/uc/item/7943f2n9>

### Author

Moukarzel, Anna Rita Eliette

### Publication Date

2023

Peer reviewed|Thesis/dissertation

Closing the Loop: Integrating Control and Sensory Feedback for Individuals with Upper  
Limb Loss and N-TMR Surgery

By

ANNA RITA ELIETTE MOUKARZEL  
THESIS

Submitted in partial satisfaction of the requirements for the degree of

MASTER OF SCIENCE

in

Mechanical and Aerospace Engineering

in the

OFFICE OF GRADUATE STUDIES

of the

UNIVERSITY OF CALIFORNIA

DAVIS

Approved:

---

Jonathon Schofield, Chair

---

Erkin Seker

---

Wilsaan Joiner

Committee in Charge

2023

## CONTENTS

List of Figures .....	v
List of Tables .....	vii
Abstract .....	viii
Acknowledgements .....	x
Chapter 1: Introduction .....	1
1.1 Motivation .....	1
1.2 Current Advanced Prostheses and Control .....	2
1.2.1 Electromyography .....	2
1.3 Nerve-Machine Interfacing and TMR .....	4
1.4 N-TMR .....	6
1.5 Sonomyography .....	7
1.6 The Kinesthetic Illusion .....	8
1.7 Objectives .....	9
Chapter 2: Establishing N-TMR for Motor Control .....	10
2.1 Overview .....	10
2.2 Methods .....	10
2.2.1 Experimental Setup .....	10
2.2.2 Experimental Protocol .....	11
2.2.3 Data Analysis .....	13

2.3 Results .....	17
2.3.1 KNN Machine Learning can Predict Motor Intent from SMG Data of the Reinnervated Muscles in Patients with N-TMR.....	17
2.3.2 Representational Dissimilarity Matrix, a Complimentary tool to Classification .....	19
2.4 Discussion .....	21
2.5 Conclusion.....	24
Chapter 3: A Vibration Movement Illusion Device for Research .....	25
3.1 Overview .....	25
3.2 Research Device Design.....	26
3.2.1 Design.....	26
3.2.2 Bill of Materials.....	28
3.2.3 Fabrication .....	30
3.2.4 Circuitry.....	35
3.2.5 Software.....	36
3.2.6 Testing.....	37
3.3 Discussion .....	41
Chapter 4: Establishing the HummingBear as a Feasible Research Tool .....	42
4.1 Overview .....	42
4.2 Preliminary Testing .....	43

4.2.1 Participants .....	43
4.2.2.A N-TMR Participant.....	44
4.2.2 Methods .....	44
4.2.2.A Experimental Set-Up .....	44
4.2.2.B Experimental Protocol.....	45
4.2.2.C Data Analysis.....	47
4.2.3 Results .....	48
4.2.3.A Able-Bodied .....	48
4.2.3.B N-TMR.....	52
4.3 Discussion .....	55
4.3.A Able-Bodied .....	55
4.3.B N-TMR.....	57
4.3.C Future Directions.....	58
Chapter 5: Conclusion.....	59
5.1 Summary .....	59
5.2 Future Directions.....	60
REFERENCES .....	61
Appendix.....	74
Appendix A: MATLAB Code and Function .....	74

# List of Figures

Figure 1. Transducer Placement on Participants.....	12
Figure 2. Experimental Set-Up with Participant's Mirroring Intended Motion.....	13
Figure 3. Ultrasound Image Thresholding Data Analysis.....	15
Figure 4. Confusion Matrices for Participant Data.....	18
Figure 5. RDM Analysis for Participant Data.....	20
Figure 6: Motor, Displacement, and Shaft Movement.....	27
Figure 7: The HummingBear and all its Components .....	28
Figure 8: Part 9 Offset Motor.....	31
Figure 9: Amplitude of Motor Shaft .....	31
Figure 10: Assembling the Shaft Subsection .....	32
Figure 11: Attaching the Motor.....	33
Figure 12: Connecting the Motor and Shaft Subsection.....	33
Figure 13: Assembling the Case .....	34
Figure 14: The HummingBear .....	35
Figure 15: The HummingBear Circuit Diagram.....	35
Figure 16: Audacity Tape Test .....	38
Figure 17: Audacity Sound File .....	38
Figure 18: Testing of Motor for Consistency with Weight and Pressure .....	40
Figure 19: Experimentation Set Up .....	45
Figure 20: Strength of Illusion.....	49
Figure 21:Range of Motion with Bicep Vibration .....	50
Figure 22:Range of Motion with Triceps Vibration.....	50

Figure 23:Range of Motion with Right Forearm Vibration .....	50
Figure 24:Range of Motion with Left Forearm Vibration .....	51
Figure 25: Ventral Forearm Vibration Sites .....	52
Figure 26: Lateral Forearm Vibration Site.....	53
Figure 27: Dorsal of Forearm Vibration Site .....	53

## List of Tables

Table 1: Participant Demographics.....	11
Table 2: Bill of Materials for The HummingBear.....	29
Table 3: Participant Demographics.....	43
Table 4: Time to Feel Motion.....	48
Table 5: Range of Motion.....	49
Table 6: Velocity of Motions.....	51
Table 7: Sensations Elicited.....	54



## **Abstract**

Our hands and arms are incredibly dexterous and capable appendages. Controlling our upper limbs requires the integration of complex descending motor control signals with rich streams of sensory information returned from the limb. Advanced bionic prostheses are rapidly advancing, however the ability to intuitively control the device and receive sensory information remains a challenge. In response to these current barriers to intuitive control and feedback, nerve-machine interfaces have emerged that can decode a user's motor intent directly from the human nervous system. However, many of these nerve-machine interfaces are experimental and may involve surgically implanted hardware, thus making this solution inaccessible to many.

Currently at UC Davis Health, many individuals with upper limb loss have been receiving targeted muscle reinnervation for the prevention of phantom and neuroma pain (N-TMR). As there is a need for pain management, N-TMR is a rapidly emerging clinical treatment for pain management done at the time of amputation. In this work, we demonstrate that N-TMR not only offers prophylactic benefits but also provides opportunities for intuitive prosthetic control and feedback. Although N-TMR is more widely accessible, it faces many challenges with current advanced prostheses. With N-TMR, there is no consideration for the depth of the muscle being reinnervated nor electrical crosstalk which can impact surface measurement techniques used for prosthetic control such as surface electromyography.

In this thesis work, we examined a novel control technique and sensory feedback method to address these challenges by employing ultrasound and machine learning approaches. Sonomyography (SMG) is an ultrasound imaging technique that applies image processing and pattern recognition algorithms to detect user's intentions from muscle deformations when a missing hand movement is attempted. We found that four participants with N-TMR surgery could

enact 4-10 hand grasps with 83.33-99.44% prediction accuracy. We also investigated how the vibration of these same N-TMR muscles could be used for movement feedback. We designed and benchtop tested a device that elicits the Kinesthetic Illusion. This illusion is the external stimulation of muscles with vibration between 70-110 Hz to activate muscle spindles. Activating the muscle spindles results in a sensation of the muscles stretching or elongating, thus participants report feeling their limb moving at the joint the muscle acts upon. We then demonstrated with five able-bodied participants and one N-TMR participant that this device can readily be used in experimental settings. Taken together, this work demonstrated that non-invasive accessible sensorimotor techniques for bionic upper limb control may be created, leveraged, applied, and adapted to the unique population of N-TMR patients.

# **Acknowledgements**

This research could not have been possible without the support and guidance of Dr. Jonathon Schofield. Thank you for the opportunity to explore what neuroengineering entails and your continuous support in my success. I appreciate all that you have given to me in spaces to learn, opportunities to grow as a researcher, and enthusiasm for exploring ways the body and robotics can communicate.

Special thanks to Dr. Joiner for your enthusiasm and support, the opportunity given to work with you and your lab has shaped my path. A big thanks to both Marcus Battraw and Justin Fitzgerald for the time spent teaching me about control systems at a level I could not have achieved on my own.

Thank you to my peers in the Bionic Engineering and Assistive Robotics lab, all who continue to inspire and support me.

A very special thanks to my family, who continue to love and support me through it all.

# Chapter 1: Introduction

The idea of what bionic prostheses can become can be seen throughout popular media such as Luke Skywalker’s intuitive and dexterous prosthesis from “The Empire Strikes Back” released in 1980 to the Winter Soldier’s cybernetic implant in “Captain America: The Winter Soldier” in 2014. An advanced truly integrated prosthesis is not just a Hollywood concept but a common goal in advanced bionics research and the clinical care of individuals with upper limb loss. With advances in mechatronics engineering, dexterous prostheses are beginning to emerge like those depicted in the movies; they are rapidly approaching the form and function of intact limbs. However, among the largest remaining challenges in limb replacement is the need for intuitive control interfaces for human-prosthesis. This includes not only the need for more sophisticated interfaces to offer natural intuitive control over the device, but also to restore sensation (sensory feedback). The latter helps close the control loop by allowing the user to feel and even embody their prosthesis as their own limb. That is, the combination of motor control and sensory feedback together offers real possibilities to promote the perception of a truly integrated limb replacement.

## 1.1 Motivation

Hands and arms are incredibly dexterous and capable appendages with 27 individually controllable degrees of freedom [1]. Efferent control signals descend from the brain to actuate muscles necessary to execute intended movements. While this happens, rich streams of afferent sensory information are returned from the limb to the brain’s higher control centers. The feedback returned is multimodal and diverse including tactile information (sensations of touch, pressure, and vibration among others), and proprioceptive (kinesthetic sensations of movement and location of body parts in space). While tactile feedback is considered a requisite for dexterous hand function

[2], proprioceptive feedback is considered vital for movements that require reaching and grasping [3], [4]. Together these sensations allow for intuitive control and the successful execution of simple through complex actions.

When an upper limb is lost, a prosthesis is often prescribed to help offset the function lost with the limb. While modern prostheses may be mechanically advanced and can offer multiple grasping movements (up to 6 degrees of freedom or more [5]), controlling these devices remains extremely challenging. With increased degrees of freedom comes a need for more sophisticated control systems to actuate the increased dexterity. Furthermore, these advanced prostheses do not offer sensory feedback. This absence one of the main factors contributing to prosthesis abandonment [6], [7]. It increases cognitive demand and requires the user to rely on visual feedback to constantly watch what the prosthesis is doing [8]. Although users may listen to sounds or feel vibration while the prosthesis is actuating, and some prostheses have added pressure sensors in the digits [9], these techniques do not replicate natural sensations. Overall, naturalistic prosthesis control and feedback remains elusive.

## **1.2 Current Advanced Prostheses and Control**

### **1.2.1 Electromyography**

Currently, electromyography (EMG) is the conventional control method for these advanced prostheses [10]. EMG records the muscles' electrical activity from the surface of the skin which can be used to decode the user's motor intent and provide corresponding control signals to the prosthesis. The stronger and more diverse the signal, the better EMG can distinguish between motor intention for dexterous, advanced, prosthetic control. Conventional EMG control uses two muscle sites [11], a technique where two sensors are applied to opposing muscle groups to map one degree of freedom to each muscle group (e.g., open/close a prosthetic hand). It has been used

for real-time control of prostheses, however, two control signals only allow for the control of two movements at a time. EMG pattern recognition is an emerging technique that has recently become commercially available and is gaining in popularity. This method consists of a series of EMG sensors placed around the residual limb. Machine learning algorithms will then recognize patterns across the electrode signals and use these to predict the user's movement intentions. Different intended movements create different patterns of muscle activity, the system differentiates between patterns and actuates a corresponding action in the prosthesis. EMG is often affected by perspiration and electrode shifting leading it to be inconsistent with signal measurement [12], [13], which is unnaturalistic control. The inconsistencies with this often-inaccurate control system leads to frustration among wearers and leads to the abandonment rate of these highly functional mechatronics [14], [15].

Most common prosthetic control techniques lack intuitive control and sensory feedback. In this thesis, we define intuitive control as the system being able to recognize one's intentions and enacting the match movement in a prosthesis. In the context of sensory feedback, we define intuitive sensation returned from the prosthesis that is experienced as temporarily and perceptually matched sensations in the missing limb. Although in conventional control systems it is possible for users to envision and attempt moving their missing limb and the system may be able to detect the pattern of activation for prosthetic control, in practice it is often not that simple.

Many hand movements use similar muscles to actuate, and when measuring muscle activity from the surface it can be challenging to measure the unique patterns for each hand motion. For example, pinch and tripod pinch both use very similar muscle groups in which their activity can be difficult to distinguish between. To compensate, many users train to map desired prosthetic motions to unique patterns of contraction, such as attempting to flex the pinky to the palm to create

a unique contraction pattern that will then activate a tripod grasp in their prosthesis. This creates an additional cognitive burden, the need for extensive training in order to effectively use a prosthesis, and departs from an intuitive control strategy.

### **1.3 Nerve-Machine Interfacing and TMR**

In response to these challenges, advanced nerve-machine interfaces have emerged that can decode a user's motor intent directly from the human nervous system. One technique that has shown promise in clinical settings, and real-world use is Targeted Muscle Reinnervation (TMR) surgery. TMR was developed for the purpose of improving myoelectric prosthetic control [16]. This procedure is performed as a secondary revision after the initial amputation surgery. The TMR procedure denervates specific native nerves that serviced the residual limb, and it relocates the severed nerves that once serviced the missing limb to strategically mapped motor branches [17]. After healing and rehabilitation, the residual limb creates unique patterns of muscle deformations when thinking about moving the missing limb which can be measured by EMG. The reinnervated muscles then act as a "bio-amplifier" to strengthen the nerve's signal for use of EMG control with prostheses. In some cases, to help strengthen the signal at the surface of the skin, layers of muscles and fat around the reinnervated motor branch will be removed to bring the signal as close to the skin as possible [18].

Since being first reported in humans back in 2004 [19], multiple studies have established TMR as a non-invasive bionic interface capable of being used in the real-world with commercially available dexterous prostheses [10], [20]–[23]. Literature highlights its potential for improved functional outcomes by having more accessible signals available for prosthetic control, and thus improving the intuitive control [24]–[26].

Further promise for TMR as a bionic prosthetic control interface has been shown in the area of sensory feedback. Of relevance to this thesis, it has been shown that kinesthetic (movement) sensation is able to be restored. The vibration of intact muscles can induce illusory movement sensations in the limb that muscle acts upon and in TMR muscle this creates sensations of the missing hand moving [27].

TMR participants have not only had access to restored sensations of movement, but also have access to cutaneous sensations [28]–[33]. The cutaneous sensations that TMR patients have described include touch, temperature, and texture of their missing limb when stimulating the residual limb [28]–[31]. TMR has even evolved to enhance these results by isolating sensory rich nerve fascicles and transferring them to strategic areas of the skin for prosthetic touch feedback. One case study had an individual with upper limb loss undergo a TMR procedure with specific sensory reinnervation for tactile sensations by isolating fascicles that had high sensory nerve fiber content from reinnervated muscles to be able to increase control of sensory feedback without interfering with motor control sites [34]. By stimulating the reinnervated sensory sites with tactile stimulation, they were able to perceive their missing hand digits [34]. Similarly, another study involved a take-home prosthesis integrated with a tactile feedback system and found their participants with TMR had an improved embodiment over their prosthesis [35]. Thus, showing that reinnervated nerves can be stimulated to elicit some of the rich tactile and proprioceptive feedback that come naturally.

Despite the encouraging results, TMR for prosthetic control and sensory feedback remains largely inaccessible to most individuals with upper limb amputation. This is because it is an experimental procedure with only a few medical centers globally offering this niche surgery to a selected few that meet the strict inclusion criteria and commitment to long term investigational



studies. Yet, intended for prosthetic control, TMR was also found to reduce chronic nerve-related pain and the formation of painful neuromas following amputation [36]–[39]. Because of the reduction of pain outcomes, a more accessible, less surgically complex variant of TMR has emerged with the prophylactic effects being the primary motivation (N-TMR).

## **1.4 N-TMR**

There are more than 2 million people living with major limb loss in the United States [39], with approximately 185,000 amputations occurring each year [40]. 35% of all amputations are upper-limb loss, with 65% being lower limb amputations [41]. 70-80% of all individuals with limb loss struggle with chronic pain such as: residual limb pain, phantom limb pain, and neuroma pain [39]. Neuromas occur at the proximal ends of severed nerves due to a disorganized growth of nerve cells [42]. The disorganized growth of nerve cells often forms painful and hypersensitive lumps of nerve tissue that commonly result in pain [42]. When it comes to traumatic injuries such as amputation, the number of severed and injured nerves leads to more discomfort and difficult pain management conditions. Due to the pain and discomfort that neuroma's cause, placing a prosthetic socket on the sore residual limb is often undesirable and can prevent the use of prostheses [42]. This further contributes to upper limb amputations having a significant impact on the individual's quality of life and functional independence.

At UC Davis Health and at a growing number of institutes across North America, individuals with amputation have increasingly been receiving targeted muscle reinnervation for the prevention of phantom and neuroma pain. N-TMR is a simplified TMR surgery derived from established TMR procedures. Because pain management is the leading motivation for TMR surgeries done today [16], the procedure is typically carried out without consideration for advanced prosthetic control. There is not a preface for usable surface signals to be able to control advanced

prostheses. This differs from conventional TMR surgery in which the procedure is conducted with the intention of reinnervation to achieve improved prosthetic control.

With no preface for prosthetic control, N-TMR participants may lack the appropriate surface-level muscle reinnervation necessary to use conventional surface-based prosthetic control systems such as EMG. In contrast to conventional TMR, current N-TMR procedures often involve surgeons reinnervating severed nerves to the single, nearest motor branch, which can be to muscles located deep in the residuum. As muscle depth and spatial orientation are not a primary motivator when selecting the muscles to be reinnervated, N-TMR can result in low signal-to-noise ratios and increases electrical crosstalk from muscle groups, as well as hindering opportunity for sensory feedback and the ability to complete neurally distinct muscle movements for prosthetic control. However, these limitations do not mean that patients who have undergone N-TMR cannot have a closed-loop control for advanced prostheses. Ultrasound technologies and the Kinesthetic Illusion hold the potential to allow for recording and stimulation (feedback) from previously inaccessible reinnervated muscles.

## **1.5 Sonomyography**

In this work, sonomyography (SMG) was utilized to collect usable signals from N-TMR muscles and demonstrate the feasibility of addressing the limitations of surface-based EMG control. SMG is an ultrasound imaging technique that detects and captures muscle activity through the depths of the residuum. It applies image processing and pattern recognition algorithms to detect user's intentions from muscle deformations when a missing hand movement is attempted. Due to SMG measuring mechanical deformation of muscle [43], it is not affected by noise and crosstalk issues that come with measuring the muscle electrical activation using techniques such as EMG. Since published in 2006, SMG systems have been reduced in dimension and cost, thus making it

a plausible system to add to prosthetic sockets [44]. Many motion artifacts, such as breathing, mechanically deform the muscle. Due to SMG measuring the mechanical deformation, we need to be certain that the system is measuring the deformation of the user's intended motion and not motion artifacts, to ensure consistent intuitive control. Studies have been done to show that SMG are aligned with user's volitional motion and not being misconstrued with muscle activity from motion artifacts such as breathing [45]. It is important to note that SMG has only been done with able-bodied participants and a limited number of individuals with amputation that have not received N-TMR [43], [45]–[48]. Additionally, work has been done to identify hand motions and their muscular deformation patterns with SMG, along with evaluating SMG's use as a control paradigm for prostheses. Thus establishing SMG as a new control system for neuro-controlled prostheses [49]–[53].

## **1.6 The Kinesthetic Illusion**

N-TMR procedures may also allow for sensory feedback to be utilized with commercially available prosthetic control systems. In this work, the Kinesthetic Illusion was examined as a way of providing movement sensory feedback to the user. The Kinesthetic Illusion is achieved in intact muscles when muscle spindles activate due to the muscles being vibrated at 70-110 Hz [54]. Muscle spindles detect the stretching of muscles. This means that activating the muscle spindles activates a sensation of the muscles stretching or elongating, thus participants report feeling their limb moving at the joint the muscle acts upon.

Throughout literature, the Kinesthetic Illusion has been studied with able-bodied individuals [55]–[71] and those who have received conventional prosthetic-focused TMR [27]. With able-bodied individuals, the Kinesthetic Illusion is a well-established, convincing, and powerful sensation that can create distortions of one's physical body and extend perceived motion

beyond physiological limits [72], [73]. Stimulating muscle spindles in the bicep and triceps can lead to the sensation of one's arm extending and flexing, respectively. Applying the vibration at one's forearm can lead to sensations of wrist motions and finger movements. With individuals who have undergone conventional TMR, when applying vibration to the reinnervated muscles, it still activates the muscle spindles, however their muscle is reinnervated with the missing hand's nerves. Therefore, they have been reported to feel missing hand motion [27], [35], [58]. When linked to a prosthesis, it can improve control, position sense, and even allow for embodiment of the prosthesis [27], [35]. Thus, integrating the Kinesthetic Illusion may be possible with N-TMR participants, and may provide opportunities for intuitive prosthetic sensory feedback.

## **1.7 Objectives**

The long-term goal of this work is to make advanced control systems more accessible for growing populations of individuals with upper limb loss receiving N-TMR surgery, and to further advance control systems for mechatronic prostheses. The objectives of this thesis work were to investigate the accuracy of SMG techniques to predict missing hand motor intentions in individuals with N-TMR, investigate the possibility of the Kinesthetic Illusion techniques as a sensory feedback method, and thus to establish the feasibility of these techniques in unlocking bionic control for individuals with N-TMR. By developing an accessible sensory-motor control interface, we may further open the doors to better understanding how natural motor-intention and sensation can be restored for prosthesis users and exploring new ways to closing human-prosthetic control-loops.

# Chapter 2: Establishing N-TMR for Motor Control

## 2.1 Overview

N-TMR has lowered the barrier to patients receiving promising pain reduction surgeries and is being widely adopted. Although the primary motivation is pain prevention and lowering the complexity of TMR procedures, there remains untapped potential for intuitive prosthetic control. The purpose of this work was to investigate the accuracy of sonomyography (SMG) techniques to predict missing hand motor intentions from N-TMR muscle displacements, and in doing so, to establish the feasibility of SMG and N-TMR for bionic prosthetic control. To detect N-TMR muscle activity at multiple levels of amputation, we hypothesize that by integrating SMG and machine learning, we can predict motor intentions from the muscular displacement captured using ultrasound imaging. The following work has been presented at the Society for Neuroscience 2022 conference and is currently in preparation for publication in the target journal: Journal of Prosthetics and Orthotics (JPO).

## 2.2 Methods

### 2.2.1 Experimental Setup

We recruited four participants through UC Davis Health who had upper limb loss and received N-TMR surgery. Participants were 39, 40, 52 and 57 years old, and two had transradial level limb loss and two had transhumeral level limb loss. All participant details are provided in **Error! Reference source not found.** Study protocols were approved by UC Davis's Institutional Review Board. Written informed consent was obtained from all subjects prior to participation in the study.

Table 1: Participant Demographics

	Participant 1	Participant 2	Participant 3	Participant 4
Age	40	52	57	39
Sex	M	F	M	M
Amputation	Left transhumeral	Left transhumeral	Right transradial	Left transradial
Tested after Surgery	18 months	6 months	34 months	48 months
Reinnervation Location	Median and ulnar nerves transferred to pectoralis minor muscle branch. Radial and musculocutaneous nerves to the serratus anterior muscle branch.	Median, ulnar, and radial nerves transferred to pectoralis major muscle branch.	Median Nerve to Flexor Digitorum Superficialis. Ulnar Nerve to Flexor Carpi Ulnaris. Superficial Radial Sensory Nerve to Extensor Digitorum Communis muscle.	Superficial radial sensory nerve to Brachioradialis muscle. Median nerve to Flexor Digitorum Superficialis muscle. Ulnar nerve to Flexor Carpi Ulnaris muscle.
Prosthesis Use	Did not regularly wear prosthesis	Did not regularly wear prosthesis	Regularly wears body powered prosthesis	Regularly wears MYO prosthetic

Participant 1 had N-TMR surgery performed three years after his initial amputation due to neuroma and phantom pain. Neuroma excision was performed as the primary repair and the freshened nerve stumps were then coapted for TMR. Participant 2 had a left arm amputation at the level of the surgical neck of the humerus. She received N-TMR surgery three months post-amputation due to severe phantom and neuroma pain. Participant 3 had a right hand near-total transhumeral amputation at the mid carpal joint. He underwent TMR at the time of his amputation. Participant 4 had a transradial amputation of the left upper extremity and received N-TMR at the time of amputation to reduce neuropathic signals that contribute to phantom pain.

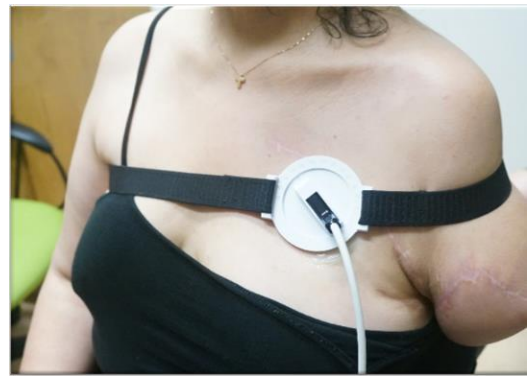
### 2.2.2 Experimental Protocol

To capture N-TMR muscle activity, we employed a Terason uSmart 3200T Ultrasound Imaging system with a 16HL7 linear array transducer (Terason, Teratech Corp, MA). Participants

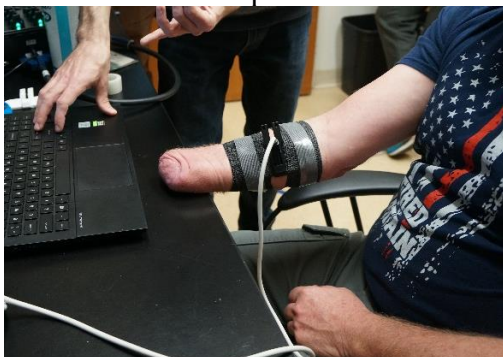
were seated in a comfortable position and the transducer was placed over the reinnervated muscles for each participant with a 3D printed housing and Coban medical adhesive to hold it in position (Fig. 1). The location of the transducer was determined by palpating the residual limb and asking the participant to contract their missing hand into a fist to first identify the general area over their reinnervated muscle groups that may be appropriate. Once identified the location was then refined by monitoring the ultrasound screen to identify the transducer placement that corresponded to the most deformation when participants attempted to make a fist.



Participant 1



Participant 2



Participant 3



Participant 4

*Figure 1. Transducer Placement on Participants: Two custom 3D printed mounts were designed for transducer placement over the chest and forearm musculature. Each participant had the transducer mounted over their reinnervated muscles.*

The images from the ultrasound system were collected at 30 frames per second with imaging depth starting at 4cm that was then adjusted as necessary for each participant. For forearm imaging, the depth was adjusted such that the ulna and radius were near the edge of the field of

view. For non-forearm imaging, the depth was adjusted such that tissue deformation during movement of the missing hand did not clip beyond the bottom of the acoustic window.

Participants were then asked to visualize and attempt to move their missing limb while mirroring the same motion with their unaffected limb (Fig. 2). Participants performed 4-10 relevant hand and wrist movements (i.e., key, pinch, point, power, tripod, wrist extensions, wrist flexion, open, thumb abduction, index flex), with 5-10 trials for each intent. Before beginning a trial, the participant was asked to relax their affected limb. Then, they were prompted to move their missing limb and hold it within a four second window. With each trial, the ultrasound imaging captured the muscle deformations corresponding to their attempts to move their missing hand. If participants reported excessive muscle or mental fatigue, the testing ended. Once complete, data processing and analysis was performed on these ultrasound image data sets as described below.

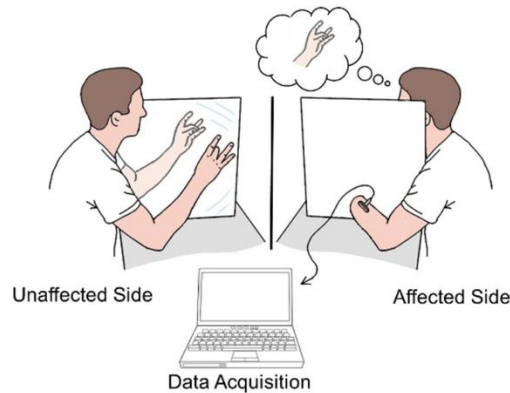


*Figure 2. Experimental Set-Up with Participant's Mirroring Intended Motion: The transducer was placed on the affected limb and the participants were asked to mirror the intended motion of their affected limb with their unaffected limb.*

### **2.2.3 Data Analysis**

The data processing was performed offline using MATLAB (R2023a, MathWorks, Massachusetts, USA). For each trial, the first frame of ultrasound data was defined as the initial muscle state (missing hand open/relaxed), with the end muscle state being an average of the last



five frames in the trial (final missing hand position). Then, using the Pearson Correlation Coefficient, a dissimilarity measurement was calculated between each frame to the initial muscle state. Image frames were down sampled to a 128x128 image. Pixels which did not deviate from their initial value across all trials were removed, and not considered in subsequent analysis. This was because we performed imaging using the trapezoidal widening of the acoustic window and captured the ultrasound data as a square matrix, some pixels were not part of the imaging at all but part of the surrounding screen/software. From here, a thresholding was performed to create a binary image, similar to a QR code, Fig. 3. To achieve this, the pixel intensity was thresholded, with the imaging grand mean equaling 2. When the pixel intensity was greater than the threshold, it set the pixel to 1. When the pixel intensity was less than or equal to the threshold, the pixel was set to 0. The end muscle state “QR codes” were then used for intended hand grasp classification.

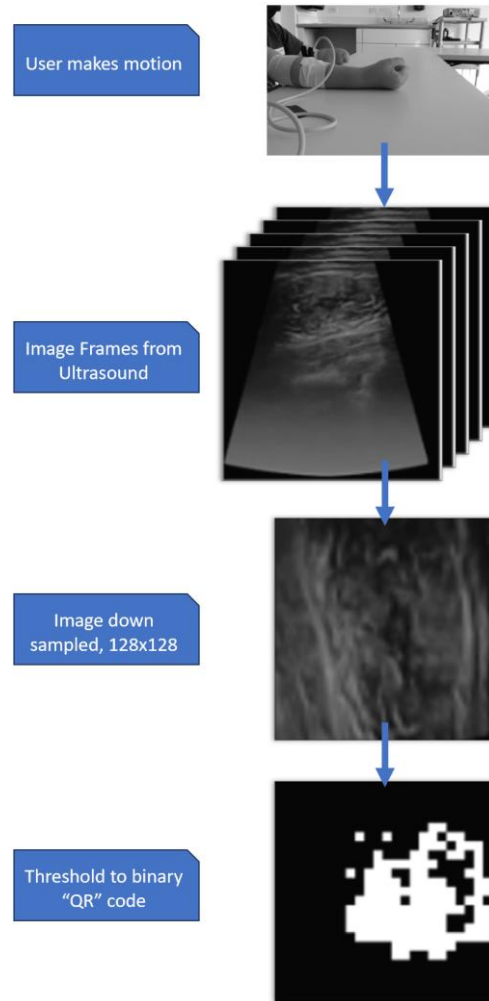


*Figure 3. Ultrasound Image Thresholding Data Analysis: When the participant thinks about making a motion, the ultrasound collects the corresponding image frames. The frames are then down sampled. From the down sample, a thresholding was performed to create a binary image to input in our machine learning algorithm.*

With our generated "QR codes," we used a K nearest neighbors (KNN) machine learning algorithm to classify each attempted hand grasp. The distance metric for KNN classification used was the Pearson dissimilarity measure done between the end muscle states. To quantify the movement prediction accuracies with the KNN, a leave-one-out cross validation (LOOCV) was performed. LOOCV is a cross-validation where one observation is removed for validation and the algorithm is trained on the remaining N-1 observations. This was done for every observation in the dataset.

The classifier analysis asks for the presence of information, and a binary yes/no is given by whether an observation is accurately classified as its true condition [74].

We also used multi-dimensional scaling to examine the trajectories of each missing hand movement. First, we calculated the pairwise similarity between each possible pair of image frames both within and across trials and across conditions to get a pairwise similarity matrix (a square matrix of size  $n\text{-Frames} \times n\text{-Trials} \times n\text{-Grasps} \times n\text{-Frames} \times n\text{-Trials} \times n\text{-Grasps}$ . For example, with 10 hand grasps, 10 trials, 4 seconds per trial at 30 fps we will have a 12000 x 12000 matrix). We then applied PCoA (metric MDS) to the pairwise similarity matrix to visualize the trajectories of the spatiotemporal muscle deformation patterns in a low dimensional space. PCoA weighs each pairwise similarity value equally when determining the low dimensional mapping. Thus, it more accurately preserves the global structure than t- distributed stochastic neighbor embedding and why we chose PCoA as our dimensionality reduction technique. This data was presented as a representational dissimilarity matrix (RDM).

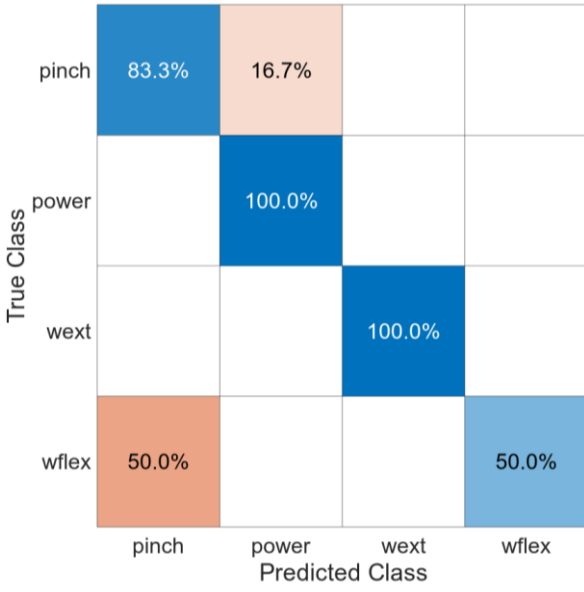
A RDM for each participant was calculated (Fig. 4). Classification analysis shows if the spatiotemporal deformation patterns are different from each other; however, classification accuracies are saturated and can only reach 100%, thus not showing how well the intra- and inter-grasps vary. The dissimilarity analysis is complementary to the classifier analysis and goes beyond asking if the data contains information about the class. It allows us to examine their variation along property dimensions of significance. The RDM analysis tool allows for a deeper look at similarity within and across grasp geometry. We used RDM to determine how dissimilar each grasp pattern was, and if each motor intent was contained within geometric structures [74].

## 2.3 Results

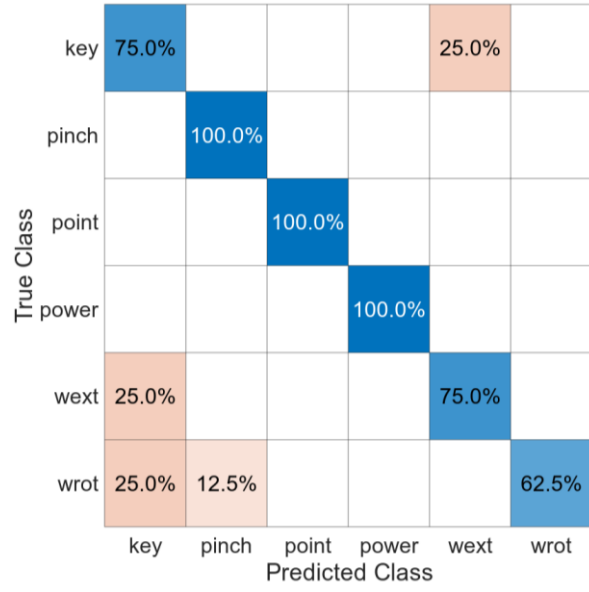
To evaluate the performance of the KNN algorithm, the classification accuracy was calculated. To examine whether participants were using a compensatory strategy to enact multiple spatiotemporal muscle deformation patterns, we used multi-dimensional scaling to examine the trajectories of each missing hand movement. A compensatory strategy is when the participant is not thinking of moving their missing limb simply as intended, rather they will contract other muscles in compensatory ways to complete the action. Take for example a participant making a pointing motion with their missing limb. Instead of just thinking about pointing their missing limb, they may tense another muscle to complete the motion. This typically occurs if users have trouble producing distinct patterns of muscle activity when attempting to move their missing hand to control a prosthesis. Thus, they learn to produce muscle activity that does not represent the actual prosthesis movement but does produce distinct and classifiable activity patterns. This is an important distinction as using compensatory strategies are a cognitively demanding and learned behavior that is rarely a naturalistic way of controlling a prosthesis.

### **2.3.1 KNN Machine Learning can Predict Motor Intent from SMG Data of the Reinnervated Muscles in Patients with N-TMR.**

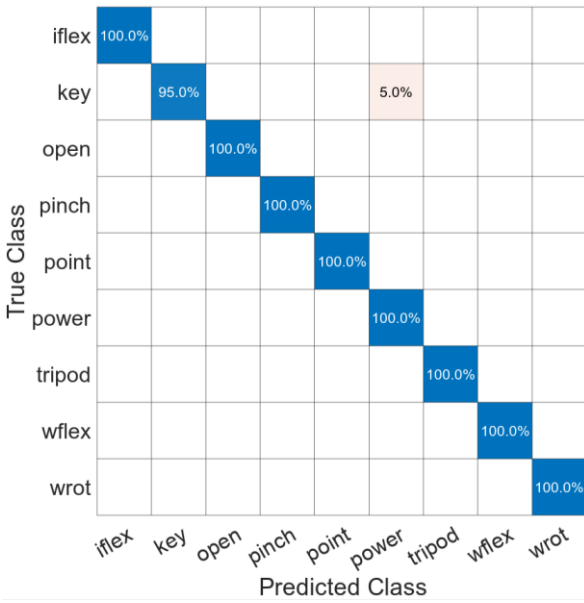
Classification analysis shows if the spatiotemporal deformation patterns are different across hand grasps. Confusion matrices for each participant were calculated to evaluate the performance of the KNN algorithm (Fig. 4). All individual intended motion predictions were above chance for each participant. Chance was calculated as 1 divided by the number of conditions. Thus, with four hand motions we had a chance percentage of 25% and with ten hand motions we had a chance percentage of 10%.



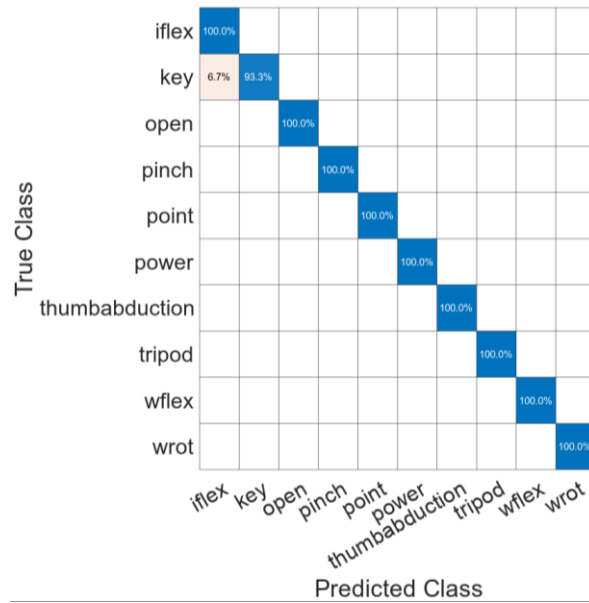
Participant 1



Participant 2



Participant 3



Participant 4

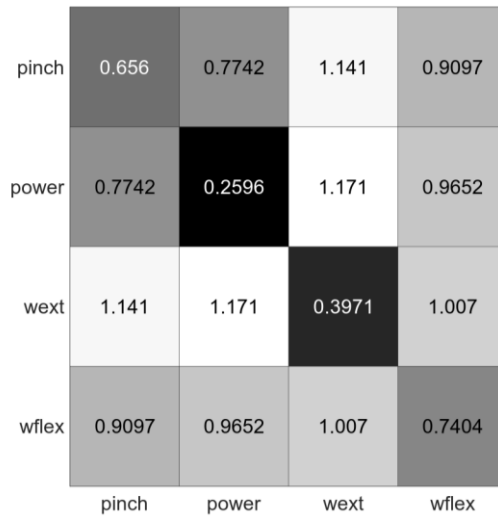
Figure 4. Confusion Matrices for Participant Data: To read a confusion matrix, the y-axis represents the true class, and the x-axis represents the predicted class. The diagonal across the matrix represents the percentage of trials that were correctly predicted.

The accuracies shown in the confusion matrices support that SMG coupled with KNN is able to consistently interpret motor intent for N-TMR participants. Each participant had a different number of hand motions due to their individual fatigue levels requiring the experiment to be

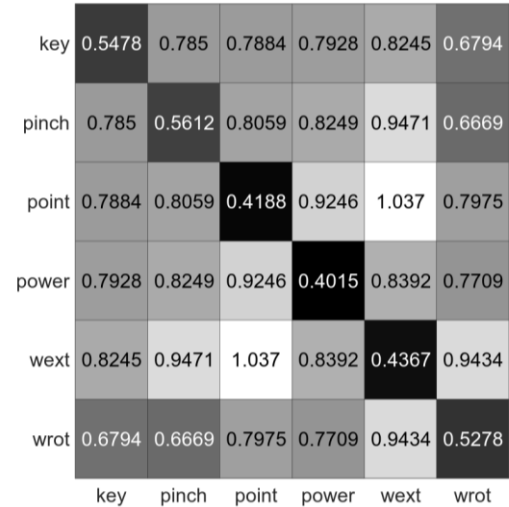
conclude at different points (more details below). For Participant 1 (four movements), the percentage of chance was 25%. With the prediction accuracy ranging from 50% to near 100%, SMG coupled with machine learning had prediction accuracies above chance for all movements. Participant 2 (six movements) had a 16.67% chance percentage, but the classifier ranged 62.5% to nearly 100% prediction accuracies, all movements predicted well above chance. Participant 3 (nine movements) had a 11.11% chance percentage and Participant 4 (ten movements) had a 10% chance percentage. Participants 3 and 4 ranged between a 95% to nearly 100% and a 93.3% to nearly 100% prediction accuracies. Thus, the lowest predicted accuracy motion per participant was still well above chance, establishing the feasibility of SMG for prosthetic control. The chance percentage varied per participant as the number of conditions varied. The predicted accuracies per each individual motion that was less than 100% could be due to the similarity of the nature of the grasp and the reinnervation sites per participant (more details below).

### **2.3.2 Representational Dissimilarity Matrix, a Complimentary tool to Classification**

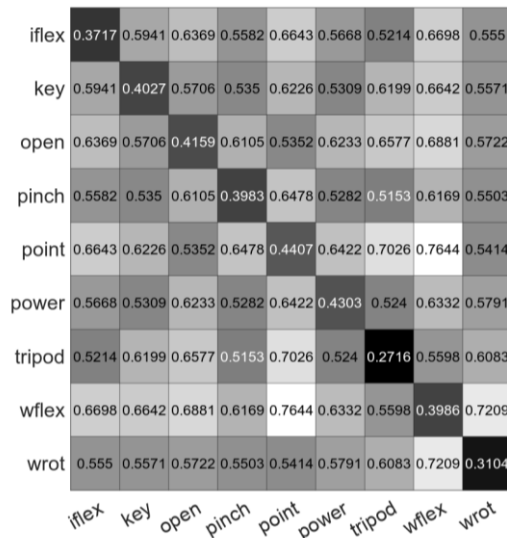
The RDM for each participant had a diagonal close to 0, showing that each intention was dissimilar to each other, Fig. 5. Each participant had a differing amount of hand motions due to their individual fatigue levels (more details below). The RDMs for each participant show how each intended motion's deformation patterns differed from one another. Through the RDM analysis, the data supports that the grasps were likely unique spatiotemporal patterns of muscle deformation, and the participants were not using a compensatory strategy to enact multiple spatiotemporal muscle deformation patterns.



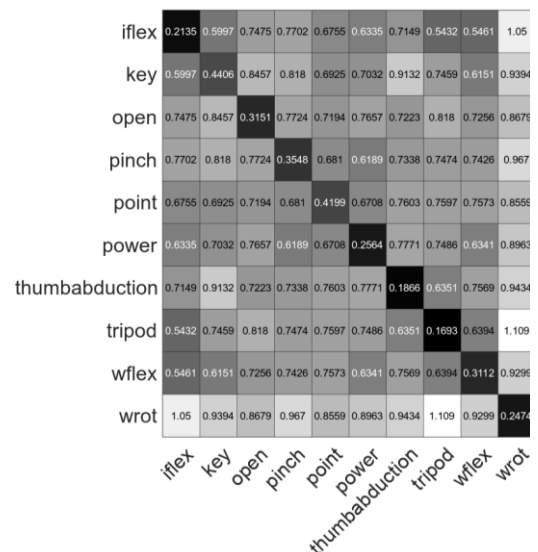
Participant 1



Participant 2



Participant 3



Participant 4

Figure 5. RDM Analysis for Participant Data: To read an RDM, each cell represents a pair of experimental conditions and the dissimilarity of the activity patterns between the two conditions. The diagonal of an RDM should be as close to 0 to show that it is perfectly correlated. The remaining square should have a value close to 1 to show no correlation with different actions.

For Participant 1, the lowest dissimilarity value was 0.2596 with the highest being 0.7404. Participant 2 had dissimilarity values range between 0.4015 and 0.5612. Participant 3's lowest dissimilarity value was 0.2716, and his highest was 0.4407. Participant 4's dissimilarity values

ranged from 0.1693 to 0.4406. Thus, establishing the feasibility of SMG for differentiating intended motions for prosthetic control.

## **2.4 Discussion**

In this work we found that patterns of muscle activation could be detected in N-TMR muscle, which can link N-TMR participant's motor intentions with the missing limb. It was also found that each muscle deformation pattern per motor intent was unique and spatially distinct from each other. This is important in terms of prosthetic control as the more diversity between inputs, the more intuitive the control system can be.

We tested a series of up to 10 missing limb movements; the variances of the movements and trials between participants were due to physical and mental fatigue reported from each participant. Although breaks were given every 2-3 minutes, Participant 1 reported a noticeable buildup of mental or physical fatigue and was not able to complete all 10 hand motions. Participant 1 stated that they did not regularly practice visualizing and moving their missing limb (a therapeutic practice known as motor imagery). This is likely why they appeared to fatigue faster than the other participants and we were only able to obtain data for four grasps. Participant 2, 3, and 4 practiced motor imagery exercises daily and did not report the task to be challenging. This was reflected in their classification results. The data suggests that individuals with upper limb loss, both transradial and transhumeral, who regularly practice moving their missing limbs may demonstrate less fatigue when operating SMG-based (or more broadly muscle-based) prosthetic control systems.

For Participants 3 and 4 the confusion matrices show that ultrasound data of the reinnervated muscles can accurately predict intended missing limb motion with an average grasp prediction accuracy of 99.39% across both participants. The RDM showed that the average



dissimilarity within each missing limb movement (ex. across all pinch grasps, across all power grasps, etc.) was lower than that between missing limb movements (ex. dissimilarity between pinch and power grasp movements). The metric MDS of the trajectories for each movement in ultrasound space are spatially separate and not parts of a common trajectory. Thus, providing evidence that patients are not using a compensatory strategy to perform unique spatiotemporal muscle deformation patterns for each missing limb movement.

While this shows promising potential of SMG for prosthetic control, it may be expected to readily detect missing-hand motions from individuals with transradial amputations as the residual muscles in their forearms were once used to actuate a hand [75]–[77]. Thus, it is not entirely surprising that we can classify motor intentions from this muscle, but we are encouraged by our findings that similar classification tasks are possible in transhumeral amputees (individuals who lost all of their forearm musculature).

However, it is important to distinguish that our team was able to use SMG to detect intrinsic hand motions in our transradial participants (motions using muscles and nerves contained exclusively in the hand if it were intact). These motions include spreading fingers open and thumb abduction. Thumb abduction is crucial to how we handle objects in day-to-day life [78], [79]. Normally, these isolated intrinsic hand motions are not possible to detect with current prosthetic control. The detection of intrinsic hand motions is an important distinction to note because the intrinsic hand muscles were lost with the hand, and it was the nerves that serviced these intrinsic muscles that were reinnervated to the forearm. Thus, we can detect movement intentions in individuals with transradial limb loss that would not be possible if not for the N-TMR surgery.

Our team also worked with individuals with transhumeral amputations, Participant 1 and 2. Individuals with transhumeral amputations have residual hand muscles and nerves reinnervated

to their chest. Individuals with transhumeral amputations face more difficulties using prostheses [80]–[82], and with SMG we can accurately classify their intended missing hand motion through the spatiotemporal muscle deformations of their reinnervated chest and trunk muscles. Participant 1 had their median and ulnar nerves transferred to their pectoralis minor muscle branch, which is a muscle deep in the residuum covered by the more superficial pectoralis major branch. Our approach captured and classified reinnervated muscle activity in this area with an 83.33% average accuracy, demonstrating the utility of SMG and its ability to measure contraction patterns throughout the depths of the residuum. Participant 2 had three individual nerves (median, radial, and ulnar), each responsible for different movements of the hand, all transferred to a single muscle motor branch servicing the pectoralis major. Having three nerves with different functions on one motor branch leads to a potential challenge because of the possibility of crosstalk where a signal sent from one nerve could interfere with the signal being sent from another on the same branch. However, attempts to move their missing hand and wrist into functionally relevant configurations still generated neurally distinct patterns of muscle activity with our ability to predict intention from these patterns with an 85.42% average accuracy, despite the reinnervation of only a single motor branch and possibility of electrical crosstalk. These average accuracies lie within the range of 66–100% found for EMG sensors [83].

Both transhumeral RDMs show higher values than transradial, however still closer to 0. This could be due to depth of reinnervation and reinnervation nerves to the same motor branch. The varying dissimilarity ranges between participants could also be due to the location of reinnervated sites and how active each participant was when thinking of moving their missing limb often. Overall, this shows that the true and predicted intentions are still more correlated to each other, and more dissimilar to other possible missing hand movements. Collectively, these findings

support the possibility of establishing SMG when used with N-TMR as an intuitive bionic prosthetic control method.

## **2.5 Conclusion**

Because the surgical priorities of N-TMR are for pain prevention, not considering control as a primary priority, it can work to the detriment of conventional surface based prosthetic control systems due to low signal-to-noise ratios and electrical crosstalk of the reinnervation sites. Investigating SMG with transradial and transhumeral N-TMR participants, we were able to classify intended motions well above chance and detect dexterous finger motions. This work provides evidence that N-TMR may be a viable bionic control modality for dexterous multi-grasp prostheses. Future directions will be to test with a larger cohort of N-TMR participants and test real time control with SMG to either virtual or physical prostheses. We are currently working on longitudinal studies which incorporate studying of long-term effects of healing time after N-TMR surgery and working on studying the learning time for N-TMR participants to control their muscles and body for intuitive bionic prosthetic control.

# Chapter 3: A Vibration Movement Illusion Device for Research

## 3.1 Overview

Modern upper limb prostheses do not offer users the ability to feel the movement of their system, a significant barrier to intuitive device control. Beyond improving device control, integrating movement feedback can also improve the integration of the user and their device by helping foster its embodiment. The Kinesthetic Illusion is a sensory feedback technique when muscles are vibrated at 70-110 Hz it activates muscle spindles, sensory receptors that detect muscle stretch. Here, the participant experiences sensations of the stimulated muscles stretching and thus, their illusory sensations of their limb moving. In individuals with upper limb amputation, vibration of residual muscles that remain after amputation can induce sensations of the missing limb moving [27], [35], [58]. While the Kinesthetic Illusion has been reported in able-bodied literature since the 1970s, current vibration devices that elicit the sensation of motion are typically designed for the purpose of rehabilitation and do not offer precise control over the vibration parameters, and thus the illusory motions that are experienced. Furthermore, to the best of our knowledge, current systems do not have integration options for data collection systems limiting their utility in research settings; all while often being cost prohibitive [84]. To study the effect of the Kinesthetic Illusion in populations of individuals with upper limb loss and N-TMR surgery, a research vibration stimulator is first needed to be designed and built. The purpose of this chapter is to describe the development of a vibration feedback system with the design motivated by considerations for research applications.

## 3.2 Research Device Design

To design a device motivated by research applications, the following criteria needed to be met: the device needs to operate at 90 Hz and a 0.5 mm peak-to-trough amplitude as previously documented to be the most effective at eliciting the Kinesthetic Illusion [27], [58]; the device needs an option to operate at a sham frequency of 20 Hz because it is outside the range of the Kinesthetic Illusion and can serve as a control to allow for the presence of vibration without kinesthetic sensations; the device needs to have integration options for data collection with MATLAB (R2022a, MathWorks, Massachusetts, USA), DAQ and motion capture hardware to use for research applications; the system needs to include a time synchronized video recorder to capture experimental activities alongside data logging; and the device should be handheld and safe to use for the participants; and the device must be less than \$500 in parts costs.

Inspired by commercially available massage guns, the HummingBear, is a research device designed under \$100 in parts costs. It consists of a DC brushless motor, an electronic speed controller (ESC), Arduino UNO, an external DC power supply, and custom 3D printed shafts, heads, and frames. Using MATLAB, the user can control the device at a sham frequency of 20 Hz or at illusion-inducing 90 Hz. Further details on the design, fabrication, and benchtop testing are provided in this chapter.

### 3.2.1 Design

The HummingBear was modeled to operate like a handheld massage gun. The design and part sizes were largely modeled considering the form factor of commercially available handheld massage guns. An Arduino controlled the electronic speed converter and motor and communicated with MATLAB. The code in MATLAB allowed the user to turn the motor on and off, as well as log video and time of the motor being activated. Through the code in MATLAB, the vibration

frequency of the motor was modified by changing the motor speed, the higher the speed the higher the stimulation frequency (described further below). The motor speed was changed by sending a value through the Arduino to the electronic speed controller, which then changed the speed of the motor to the desired value. Once activated, the motor rotated and was connected to a displacement piece and a shaft. The HummingBear had the rotation of the motor offset by a displacement piece. The displacement rotated with the motor. When the shaft was connected to the displacement, it moved in a straight-line forward and backward by constraints of the casing, Figure 6. Because rotational movement was being converted to linear movement, the shaft moved the distance of the displacement from the motor. The displacement correlated to the amplitude of the shaft's movement. Figure 7 shows the HummingBear in its completed form and in an exploded view with all its components. The red balloons on each part correspond to the bill of materials provided in Table 2.

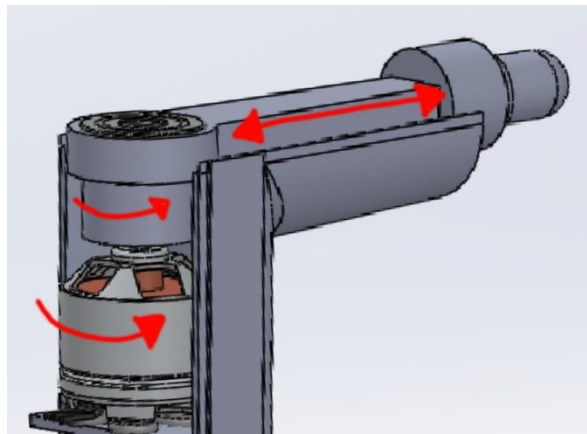


*Figure 6: Motor, Displacement, and Shaft Movement*

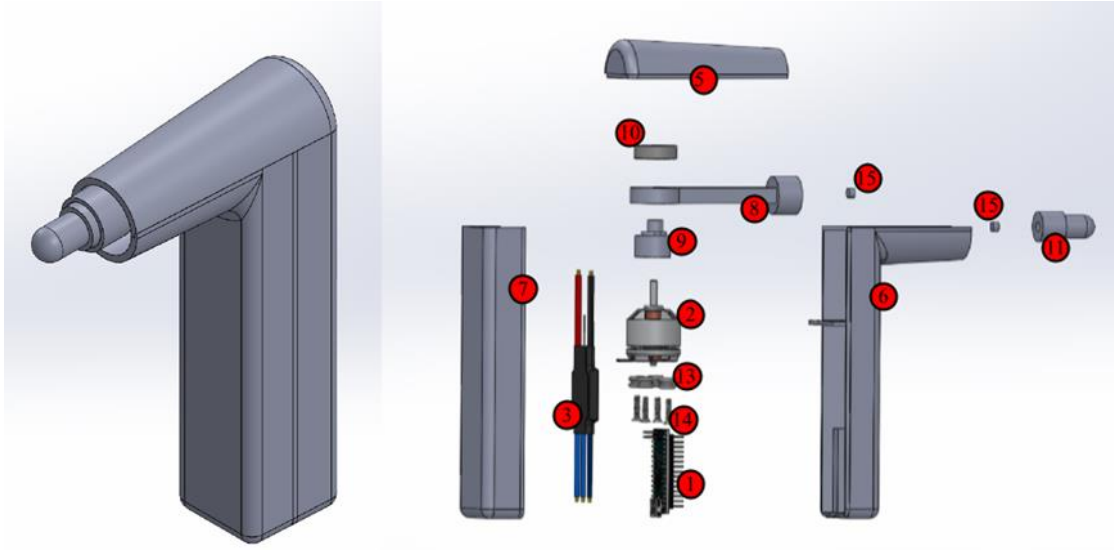


Figure 7: The HummingBear and all its Components

### 3.2.2 Bill of Materials

Table 2 below is the bill of materials. Many prices shown are for the quantity of the part per unit price, such as the cost of the PLA plastic used in printing. Using the CAD models, a conservative estimate of the mass for all printed parts was found at 74g. The weight was then factored from a 1000g spool of PLA with a cost of \$20.99. From this spool, 74g cost \$1.56. This was done for all parts that come in a unit with larger quantities, Parts 12-15. The total cost of the HummingBear came to \$95.97, well below current pricing rates for a similar research and clinical device.

Table 2: Bill of Materials for The HummingBear

Part Number	Subsection	Part Name	Description	Fabricated/Purchased	Quantity	Price/Quantity
1	Circuitry	Arduino Nano	used to control and communicate with the device, it is the hub for all electronic components	Arduino	1	21.8
2		850KV Brushless DC Motor	used to stimulate a vibration with an up down motion, a DC brushless motor was used because conventional massage guns utilize this motor	Amazon	1	17.99
3		30A ESC	used to model the brushless DC motor as a servo, to control the rpm of the motor, and thus the frequency	Amazon	1	16.99
4		3-24V 2A DC Power Adapter	used to power device	Amazon	1	14.99
5	Casing	Top Casing	covers the part where the Motor Shaft goes and helps guide it straight	Fabricated	1	
6		Bottom Front Casing	this is the front casing that has the motor holder and the Arduino holder with an extruding design to help guide the shaft to move straight	Fabricated	1	
7		Bottom Back Casing	this is a simple backing for the device with no enclosure for the ESC	Fabricated	1	
8	Shaft	Motor Shaft	a simple shaft modeled after a massage gun's shaft. It is made to fit a bearing and has a pre-fit head holder	Fabricated	1	
9		Motor Displacement	mechanically offset rotation to be 0.5mm. It is pressure fit into the motor shaft and displaces the motor. It connects to the bearing and shaft to cause the 0.5 amplitude	Fabricated	1	
10		608-2RS Bearing	1 bearing pressure fit into Motor Shaft and used to help with rotation and connection to the motor and motor displacement	Amazon	1	0.9
11		Head	the head of the device that protrudes into the body. It is designed to be easily changeable and magnetically connected with the head holder designed in the shaft	Fabricated	1	
12	Hardware	PLA	material used to 3D print and develop casing and shaft system	Amazon	74g	1.56
13		1/4" Rubber Grommets	4 grommets used to support motor and help silence noise	Amazon	4	0.19
14		4-40 Flathead Screws	4 screws used to stabilize motor to casing	Amazon	4	0.13
15		Mini Magnets	2 magnets used to allow for easy interchangeability between Head and Motor Shaft parts	Amazon	2	0.07
16		Velcro Straps	used to make sure all casing parts are secured together	Amazon	1	3.85
17		USB-A to USB mini-B	used to connect Arduino Nano to computer	Amazon	1	3.82
19		Banana Plug Converter	used to connect ESC to DC Power Adapter	Amazon	1	7.99
18		Super Glue	used to glue grommets for silencing, and to make sure Bearing, Motor Displacement, and Motor Shaft are all connected securely	Amazon	1	5.69
Total Cost:						95.97



As this device will be used with human participants, the DC power source and device was used with an 1800W TRIPP-LITE electrical risk medical grade isolation transformer to protect the participants from possible electrical hazards by isolating the electrical circuit to prevent electrical current from passing through their body.

### **3.2.3 Fabrication**

For this device, components were either fabricated or purchased from any store that sells hardware and electronic components. All fabricated components, parts 5-9 and 11 as seen in Figure 5 and Table 2, were 3-D printed with PLA at an infill of 20%. Parts 5,6 and 8 were printed with supports to ensure the quality of the device. Printing with supports prevented the deformation of overhanging aspects of the design by giving a surface area for the layers of the part to print on. The purpose of 3-D printing with PLA was to ensure the final vibration device was cost effective and manufacturable in most research laboratories. 3-D printing with PLA also allowed for the simplification of replacing parts if any were to break, wear out, or if modification of certain parts were necessary in future research applications. The Motor Displacement can be changed by replacing Part 9 to adjust the motor offset, thus creating a vibration amplitude greater or less than 0.5 mm if required in future applications. Part 9 mechanically controlled the amplitude by connecting to the motor with an offset fitting from the center. By controlling how far the offset is, the radius of the movement of Part 9 becomes the distance of the offset. Currently, the motor was offset 0.5 mm by Part 9, and the Motor Shaft, Part 8, connected to Part 9, moved 0.5mm forward and 0.5 mm backward as a result. Figure 8 shows the offset of the motor from Part 9 and Figure 9 shows the amplitude of the Motor Shaft, with the displacement. Part 11, the Head, can be changed to any shape that the researcher would like to interface with the participant's skin.

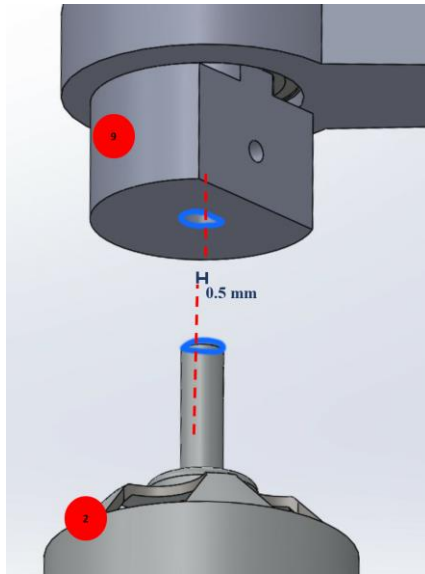


Figure 8: Part 9 Offset Motor

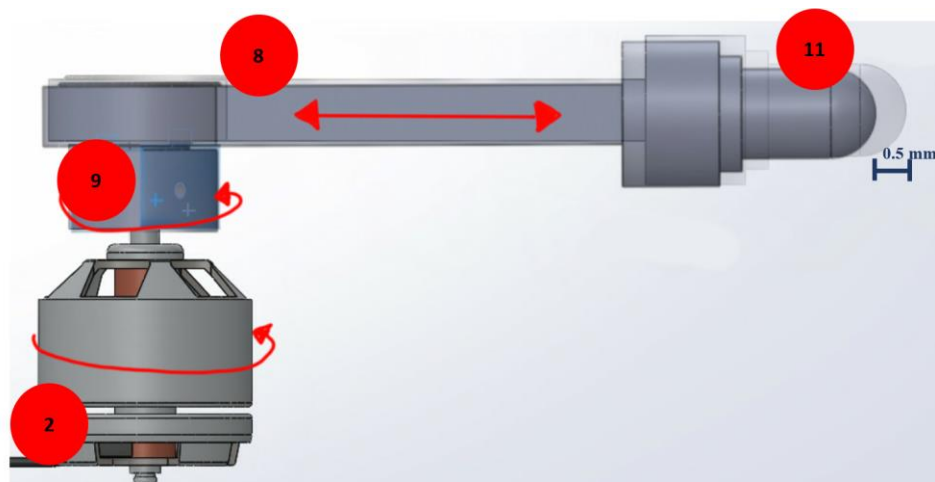
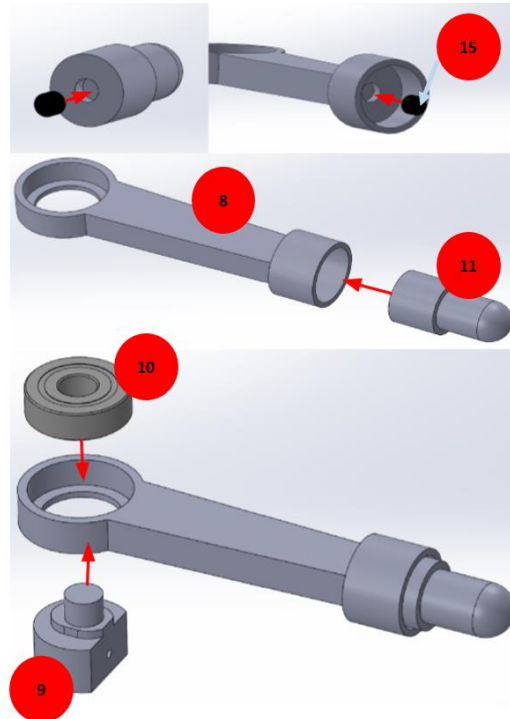


Figure 9: Amplitude of Motor Shaft

Once all parts were 3-D printed and purchased, the device was assembled. The order that the device was built was: solder the circuitry, assemble the shaft subsection, attach the motor to the casing, attach the shaft subsection to the motor and assemble the casing (described below).

The circuit was soldered together, and the diagram is referenced in Figure 15. The shaft was assembled by first supergluing a magnet into Part 8, the Motor Shaft, in the head holder area and into Part 11, the Head, so they can connect to each other. Then the plastic in Part 8 was heated, where the bearing, Part 10, should fit, and the bearing was pressure fit in. Superglue was added to

the inner sides of Part 8 where the bearing will be pressure fit for added assurance that the bearing will not pop off during testing. Finally, Part 9 was pressure fit into the center of the bearing from beneath the Motor Shaft and bearing assembly by similar means. Part 9 was heated and covered in superglue to ensure a tight fit. How the pieces fit together can be seen below in Figure 10.



*Figure 10: Assembling the Shaft Subsection*

The motor was attached to the casing with four 1/4" rubber grommets and four 4-40 flat head screws, Figure 11. The length of the screws was measured with the motor to see how much to shorten the screws and cut them to size. Then using Part 6, the Bottom Front Casing, the motor was lined with the predesign screw holes in the motor stand. Before screwing the screws, the rubber grommets were placed on top of each hole and the motor was placed on top of the grommets. Finally, they were both screwed in place from under the motor stand. The purpose of the rubber grommets was to elevate the motor as it was not flat and domes out, allowing reduced friction

between the motor and plastic. With reduced friction, it silenced the device and prevented any stalling that could occur if the motor wore into the plastic.

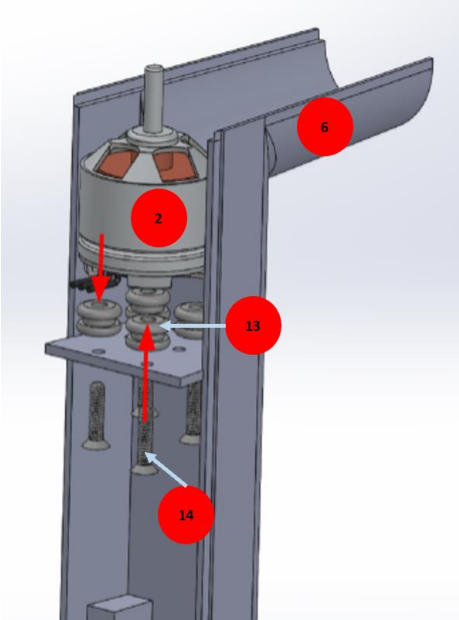


Figure 11: Attaching the Motor

The shaft subsection was attached to the motor by heating up the motor displacement piece and pressure fitting the hole to the motor’s shaft. Superglue was placed around the motor’s shaft to ensure a secure fit. This connection can be seen in Figure 12 below. Note that the motor shaft needed to be filed and Part 9 needed to be shortened to line up the shaft with the protruding section of Part 6.

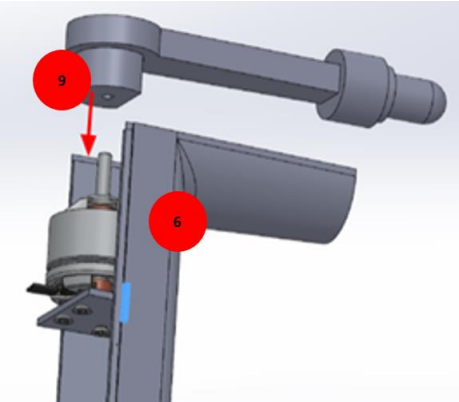


Figure 12: Connecting the Motor and Shaft Subsection

Finally, the casing was assembled, Figure 13 and 14. First, the Arduino Nano was fit into its allotted space in Part 6 and the ESC was arranged on Part 7, Bottom Back Casing, so that it snapped together. There are lips and grooves on Parts 5,6, and 7 to help snap the casing together. Then Part 5, the Top Casing, was added to the assembly. To secure the casing, Velcro loops were added around the handle of Part 6 and 7 and around Parts 5 and 6.

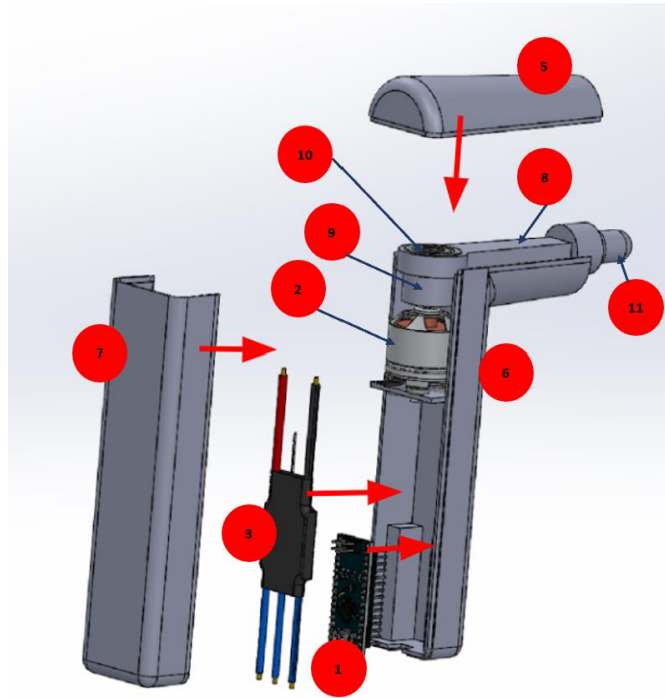


Figure 13: Assembling the Case

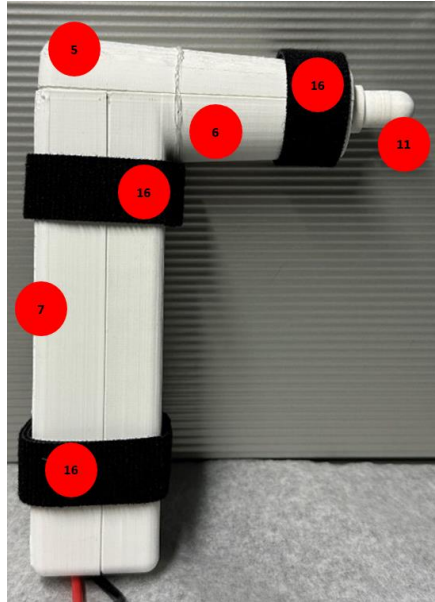


Figure 14: The HummingBear

### 3.2.4 Circuitry

The Arduino Nano, ESC, brushless motor, and DC power adapter need to be able to communicate with each other. To connect the hardware together, Figure 15 below shows the wiring diagram.

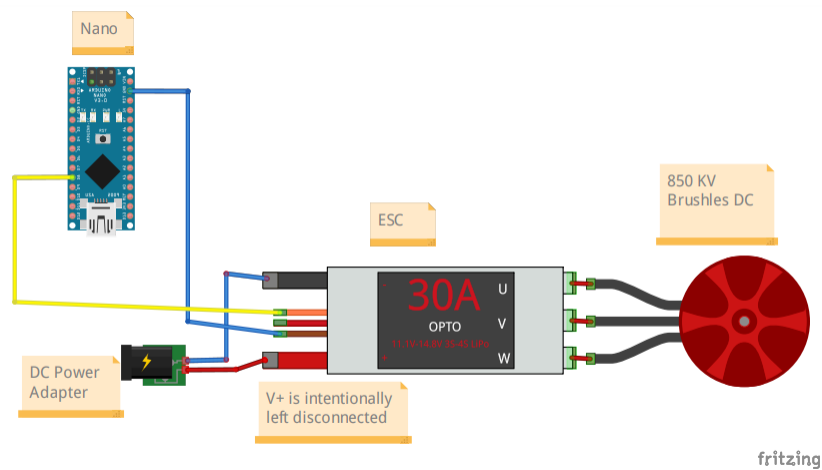


Figure 15: The HummingBear Circuit Diagram

The output voltage (V+) is intentionally left disconnected as the Arduino Nano does not have enough power output at 5 V to meet the combined demands of the ESC and motor. The ESC

is to control the rotation and speed of the motor by communicating between the battery and motor to create the speed of the rotating magnetic field in brushless DC motors to make the motor rotate at certain frequencies. This design allows all power to be drawn from the external DC power adapter. From here the Arduino Nano then communicates with the computer via a USB-A to USB-mini-B cable.

### **3.2.5 Software**

The software being used was MATLAB. Within MATLAB, the Arduino support from MATLAB library (R2022a, MathWorks, Massachusetts, USA) was added to be able to communicate with the hardware from one software source. Two files are needed to run the device, “Movement\_Vibration\_Illusion.m” and “Vibration\_Function.m” and can be found in Appendix A. “Movement\_Vibration\_Illusion.m” is the main interface where the user can input the folder name for the test and participant and control the device between 20 and 90 Hz. Once the user inputs their desired vibration frequency, “Vibration\_Function.m” is called. The purpose of “Vibration\_Function.m” is to control the motor. Once called, the code will ask the user to press “enter” to start the device. Once the device is running (vibrating at the user define frequency), a web camera will also begin to record, and a stopwatch will record how long the device is running. The user can press 0 at any time to end. If the user presses any key besides 0, the code will save the time stamp and add it to a table. This way the user can flag any time that may be relevant to the experimental results and can link the event to the video recording. Once the user stops the device, they will be asked to name the trial and if they want to continue to a new trial. If they choose to continue to a new trial, the function will repeat, and the user can begin the trial at the current frequency. If the user chooses to not continue to the next trial, “Vibration\_Function.m” will end and return the user to “Movement\_Vibration\_Illusion.m”, where they can decide to switch

frequencies or end the code. This code is modeled to be run simultaneously or added to prosthetic control software that is currently being used in the Schofield laboratory. Its ability to track time in relation to video and its ability to be integrated with current control code make it a data syncing device.

### **3.2.6 Testing**

While building the device, testing needed to be conducted to ensure the HummingBear vibrates at the appropriate frequencies, does not stall with load applied to the stimulation head, and operates at appropriate voltage levels making it safe to use to avoid motor burnout and electrical shock. To do so, the HummingBear was tested periodically as device development was carried out.

To ensure that an 850 kV brushless DC motor can output the appropriate frequencies, the range of RPMs the motor can output were tested. The first test was performed with the circuitry already wired on a breadboard with an external DC power supply. The voltage was set at 7.4 V as that was what the motor manufacturer rated it for. The current used was well below 1A, averaging around 0.3 A. Using MATLAB, a series of positions between 0 and 1 were inputted to the motor to represent the position and RPM speed. To calculate the RPM, an adhesive tape strip was added to the motor's shaft and an audio recording was taken to capture the sounds the tape made while striking a surface while the motor was rotating. This can be seen in Figure 16. Once recorded, Audacity (3.3.3, Muse Group, Russia), an audio editing software, was used to measure the time duration it took for the motor to make one revolution from peak sound to peak sound. An example of the sound file can be seen in Figure 17. With that value set, the seconds were converted to minutes to calculate the RPM. From here, the RPM was converted to Hz, the unit for frequency, by dividing by 60, as there are 60 RPM for each 1 Hz. This was done five times per recording, with five recordings done at the RPM found for 90 Hz and 20 Hz. The average for the tests at 90 Hz



was 89.98 Hz with a standard deviation of 0.99. The average for the tests at 20 Hz was 20.30 Hz with a standard deviation of 0.41. This gave the preliminary positions for the motor. It was found that an 850 kV was best to reach 20 Hz and 90 Hz. Motors with higher kV's could not reach an appropriate sham frequency range.

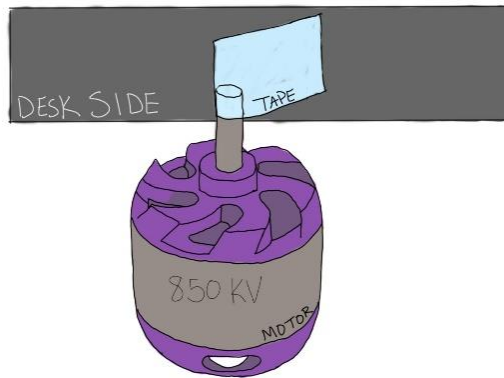


Figure 16: Audacity Tape Test

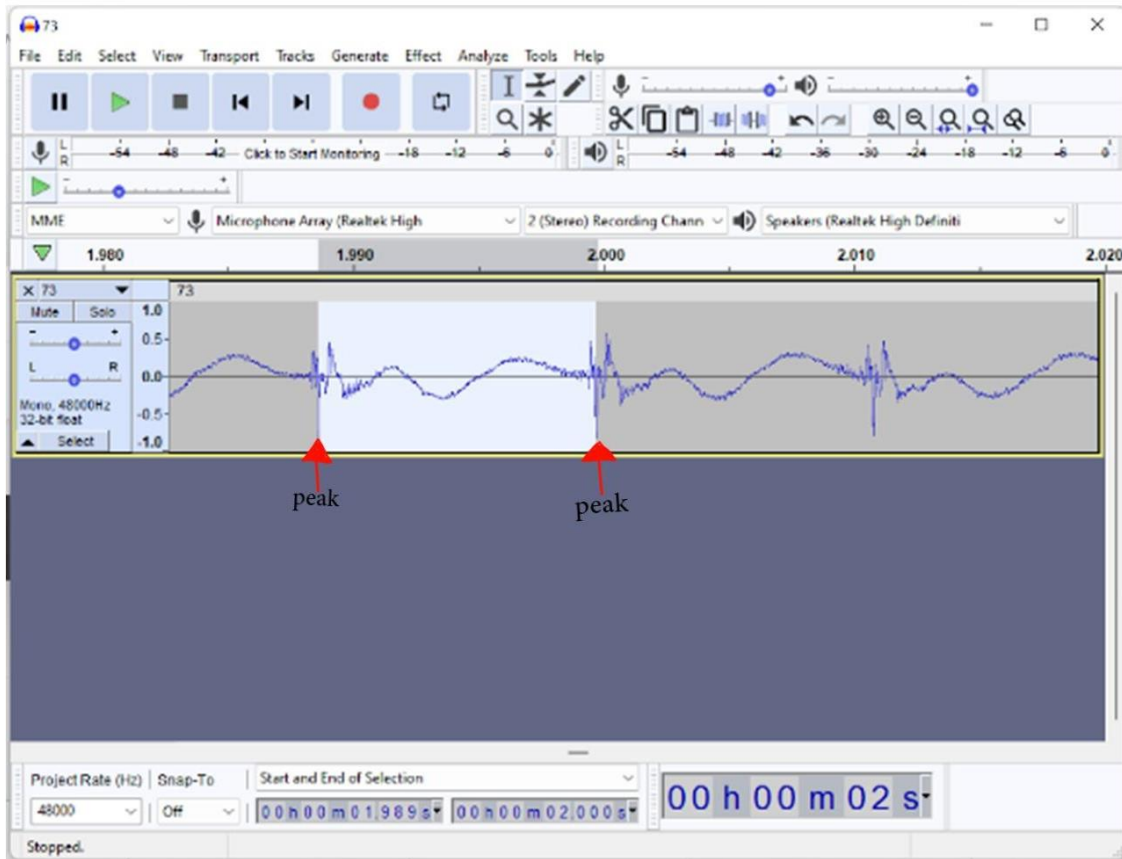


Figure 17: Audacity Sound File

While validating that the motor capable of achieving the range of frequencies required for the Kinesthetic Illusion and a sham frequency, the next test was to evaluate the motor's frequency under load. The second test was to ensure that the motor would not stall with added weight from the shaft subsection and added pressure from being pressed into a participant's arm. This test was done by drawing a black line on the Motor displacement, Part 9, and placing the shaft into two human participant's ventral forearm. This set up can be seen in Figure 18. The motor was then run at each noted motor position from the first RPM test conducted, mentioned above, and recorded. The video was then opened on a video editing software, VSDC (8.1, ADP-RB LTD, Russia). From here, frame-by-frame analyses were performed to note how long it took for the black line to complete one revolution. The frames were recorded at 180 fps to make sure aliasing effects were not captured. The frames were then converted to seconds, the seconds to RPM, and the RPM to Hz as mentioned in the earlier test. Frames from the video were taken in 30 second intervals and measured to ensure that the motor output had a consistent RPM and did not stall. From these sections, the number of frames it took for the black line to complete a rotation were documented and converted to Hz. As done before with the first test to ensure the motor's capability of operating at the appropriate frequencies, this was done five times per recording, with five recordings done at the RPM found for 90 Hz and 20 Hz. The average for the tests at 90 Hz was 90.02 Hz with a standard deviation of 0.95. The average for the tests at 20 Hz was 20.19 Hz with a standard deviation of 0.63. This test confirmed that with added pressure from an arm and weight from the bearing and motor shaft subsystem, the motor would still output the appropriate frequencies consistently.



*Figure 18: Testing of Motor for Consistency with Weight and Pressure*

The objective of the third test performed was to confirm that the motor was drawing consistent power and the external power supply purchased for the device was outputting consistent and appropriate power.

By adding a voltage reader to the circuitry, the voltage output from the circuitry remained between 7.42-7.48 V, while running continuously for one hour unloaded. This fell within the manufacturer range of 7.4-12 V. A voltage reader was also connected to the purchased DC power supply to validate that it can output 7.4 V consistently. When the bought DC power supply was set to 7.42 V for two hours, the voltage reader read a range of 7.4-7.48 V. The DC power supply was tested disconnected and connected to the circuitry unloaded, each for two hours, to confirm its consistent and appropriate voltage output between 7.4-7.48 V.

The final test was to design ensure that the device would run consistently during a test without overheating and stalling. To do so, the second and third test were combined. The voltage reader was set up with the circuitry and a video was capturing the rotation of the black line on the motor displacement. A typical test with a participant will be within two hours, and not have the

motor continuously running within the experiment. Therefore, to ensure the device will function as intended within the 2-hour experiment, a conservative test under extreme demands was run at four hours. The voltage reader showed an appropriate range of values between 7.42-7.48 V, which fall within the manufacturer range of 7.4-12 V. The video footage was reviewed to verify the consistency of the vibration amplitude and displacement.

The results of these tests confidently confirm that the device operates consistently as intended and within manufacturer's guidelines, making it safe to use for data collection with humans.

### **3.3 Discussion**

The HummingBear is a cost-effective data syncing research vibration device. With the HummingBear, researchers can go “under the hood” and readily adjust vibration parameters and integrate the system with a variety MATLAB compatible data acquisition or prosthesis control systems. The science that increasing the accessibility of a vibration research device enables will lead to a deeper understanding of the Kinesthetic Illusion and lower a barrier to the application of vibration induced movement illusions as a kinesthetic sensory feedback technique for prosthetic control. Currently, the design of the HummingBear is being refined and we are preparing documentation, a bill of materials, and all print files for an open-source release.

# Chapter 4: Establishing the HummingBear as a Feasible Research Tool

## 4.1 Overview

The purpose of this work was to establish the feasibility of the HummingBear as a research device capable of eliciting the Kinesthetic Illusion by recruiting a small cohort of able-bodied individuals and one individual with amputation and N-TMR surgery. The kinesthetic illusion occurs when vibrating muscles between 70-110 Hz. This stimulus can activate muscle spindles, which are small sensory organs present in the muscles that are responsible for detecting muscle stretch. Their activation creates the illusion that the stimulated muscle is being stretched and this is experienced as motion in the joint that the muscle acts upon. Thus, when researchers target certain muscle groups, it can be predicted what the average sensation and motion will be. For example, when targeting the biceps, it is common to feel the arm extending, whereas targeting the triceps most typically feel like the arm is flexing [54], [64], [67], [71]. When targeting the forearms, there are multiple muscles that work in coordinated ways to actuate the highly dexterous hand and wrist. Thus, singling out an individual muscle for vibration stimulation is very challenging. As a result, we typically find that larger whole-hand and wrist movements can be elicited as opposed to more specific sensations such as movement of a single digit. Conventionally, there are sensations of wrist rotation inward (pronation) and outward (supination) from stimulating the outer forearm and inner forearm, respectively [85]. With TMR participants hand nerves are reinnervated to the residual muscle; therefore, when the Kinesthetic Illusion was applied with TMR participants, they reported sensations of missing hand motions, as well as demonstrated improved prosthetic control and position sense of their prosthesis [27], [35], [58]. While with able-bodied individuals, one can predict intended sensations when stimulating targeted sites; with TMR individuals, the location

and sensations of each targeted site differs per individual and is dependent upon the nerves that were reinnervated to each residual muscle.

**The goal of the work described in this chapter was to investigate how effective the HummingBear was at eliciting the Kinesthetic Illusion in able-bodied cohorts and an individual with N-TMR.** We cataloged and compared their experienced movement sensations with those currently reported in literature to ensure the HummingBear could induce the Kinesthetic Illusion in cohorts of experimental subjects.

## 4.2 Preliminary Testing

The testing and protocol have been approved by UC Davis’s IRB, number 2043447-1. All subjects provided written informed consent prior to participating in this work.

### 4.2.1 Participants

Five able-bodied participants and one participant with transradial limb loss and N-TMR surgery were recruited. Able-bodied participants were chosen for this testing to examine how well the device was able to induce its intended function of eliciting the Kinesthetic Illusion. Participant demographics can be seen in Table 3.

*Table 3: Participant Demographics*

Participant Number	Gender	Age	Notes
1	M	23	Healed Torn rotator on Left Shoulder
2	M	22	Healed Nerve damage on Left Shoulder
3	F	22	
4	M	28	
5	M	31	
N-TMR	M	58	Right Transradial Amputation

All able-bodied participants were tested by vibrating their left arm, the non-dominant arm, and the N-TMR participant had their affected limb vibrated. The non-dominant arm was stimulated as

previous documentation indicates non-dominant arms rely more on proprioception sensations and lead to more vivid sensations of proprioceptive illusions [86], [87].

#### *4.2.2.A N-TMR Participant*

The N-TMR participant was a 58-year-old male with a right hand near-total transradial amputation at the mid carpal joint. He underwent TMR at the time of his amputation. He had his Median Nerve reinnervated to the Flexor Digitorum Superficialis, his Ulnar Nerve to the Flexor Carpi Ulnaris, and his Superficial Radial Sensory Nerve to the Extensor Digitorum Communis Muscle. He was tested 43 months after his amputation and N-TMR surgery.

### **4.2.2 Methods**

#### *4.2.2.A Experimental Set-Up*

The experimental set up was modeled after previous literature reporting on similar experiments [27], [58]. The goal of the experimental set up was to capture the movements of participants' unstimulated limbs, as they would be demonstrating the sensations they were experiencing with this limb. The materials required to test were a computer, a video recorder, GoPros, the HummingBear, foam blocks, an arm rest, a blindfold/sleeping mask, felt tipped markers, and baby wipes. The computer, camera, and HummingBear were used for data collection. The computer controlled the HummingBear and camera. The video recorder was set to record the unstimulated limb to capture their mirrored sensations. The computer turned on the HummingBear and camera such that when the HummingBear's motor was on, the camera was recording, and when the motor was off the camera was off. This gave the ability to video capture experimental activities synchronously with the activation of the experimental equipment. The HummingBear stimulated the participant to elicit the Kinesthetic Illusion. The GoPros were placed around the room and participant to document the experimental session and record participant descriptions of

the sensations they experienced during the testing session. The foam blocks and arm rest were to rest the arm on, allowing the participant to relax and sit comfortably during testing. The blindfold/sleeping mask covered the participant's eyes to help facilitate the illusion; visual information can diminish the illusion [88]. The felt tipped markers were used to draw on the participant's body where we vibrated and where they felt relevant sensations of limb motions. Finally, the baby wipes were used to clean the felt tipped marker off the body at the end of the testing session.

Despite the fact that the HummingBear does have a sham (20 Hz) vibration setting, for the purpose of this experiment, we only used 90 Hz vibration to examine if sensations of motion can be elicited. (90 Hz has been shown to consistently elicit strong and convincing illusion in prior literature [58], [89]). Figure 19 illustrates the experimental setup.



*Figure 19: Experimentation Set Up*

#### *4.2.2.B Experimental Protocol*

The following steps were followed to conduct the experiments:

1. The participant was positioned such that their limb was rested and the muscles that were stimulated were accessible with the HummingBear.
  - a. At each arm position, the tendons in the bicep, triceps, forearm were vibrated.



2. The motor ran continuously for 5-15 minutes within the same muscle group. Each location was vibrated for approximately 45 seconds before moving to the next location within a radius of approximately one inch of the first vibrated site. The first vibration site was chosen by asking the participants to flex while palpating their limb to feel where deformation of muscle occurred. The strongest area of deformation was chosen as the first location. Within the first five minutes, the participants were not made aware that we were vibrating to achieve movement sensations. They were only asked to report any sensation they felt.
  - a. They were asked to describe anything that did not feel like a simple vibration.
    - i. A second investigator was present to document what the participant was reporting. This included the sensations they reported experiencing and the time at which they occurred. They documented the location number of the vibration and transcribed the participant's descriptions. They noted how convincing the sensation was and what motions were described.
  - b. When a movement sensation was experienced, the participants were asked to demonstrate any sensations with their unstimulated side.
3. When the participant began to report sensations beyond simple vibration, the second investigator documented it.
  - a. When they reported sensations of their limb moving, the following questions were asked:
    - i. Can you show the sensation with the other hand?
    - ii. How fast is it moving?

- iii. How convincing is it that the hand is moving from 1-5? 1 being not at all and 5 being extremely [58]?
4. When they mentioned that they were experiencing a sensation beyond simple vibration, the location of stimulation was marked with a felt tipped marker. When finished with the experiment, the marks were photographed prior to being cleaned off the participant with baby wipes.

Throughout the experiment, the participants were reminded to stay relaxed. Breaks were taken when needed by the participants to help relax their muscles. The sessions ranged between 1-2 hours depending on the amount of breaks needed.

#### *4.2.2.C Data Analysis*

The data analysis consisted of documenting the time duration it took for participants to first feel the kinesthetic illusion, the perceived strength of the illusion, the range of motion of each illusory movement, and the velocity each illusory motion had for the participant [58], [66], [90]. Once the sensation of motion was established, the participants were asked then to rate the convincingness of the illusion [58] on a scale of 1-5 Figure 20. To determine the range of the motion, the participants used their unstimulated side to demonstrate the distance of the illusory motion they experienced. The angular displacement as measured from their rested position to the final position where they felt their limb move in space, (Table 5 and Figures 21-24). The resting and final position were taken from anatomical landmarks within the video footage of the experiment. The velocity of movement sensations was calculated by dividing the range of motion by the time it took to complete the motion. This analysis was performed at the locations where the participants reported the sensation to be most convincing. These locations were identified after first exploring the limb to identify locations eliciting movement sensation and then we returned to

each location asking participants to rate the convincingness of the illusion as described above (Table 6).

### 4.2.3 Results

#### 4.2.3.A Able-Bodied

Consistent with prior work [58], [66], [90], the data presented here include the time duration it took for participants to first feel the kinesthetic illusion, the perceived strength of the illusion, the range of motion of each illusory movement, and the velocity each illusory motion had for the participant. The first time a participant experienced sensations that were beyond simple vibration were documented and can be seen in Table 4. This data was extracted from the video recording of testing sessions.

Table 4: Time to Feel Motion

Participant	Time (min)
1	0.5
2	0.8
3	2.3
4	No Illusion
5	No Illusion
Average	1.2

The average time for all participants to first experience movement sensations was 1.2 minutes. This is within the range of time to feel the sensation of motion as previously documented to be within the first 5 minutes of testing [58]. Participants 4 and 5 did not experience the Kinesthetic Illusion.

Once the Kinesthetic Illusion was first experienced, all able-bodied participants were asked to rate the convincingness of the illusion on scale from 1 to 5. Participants 1-3 reported the convincingness of the movement illusion to be between 4 (very) and 5 (extremely), Figure 20.

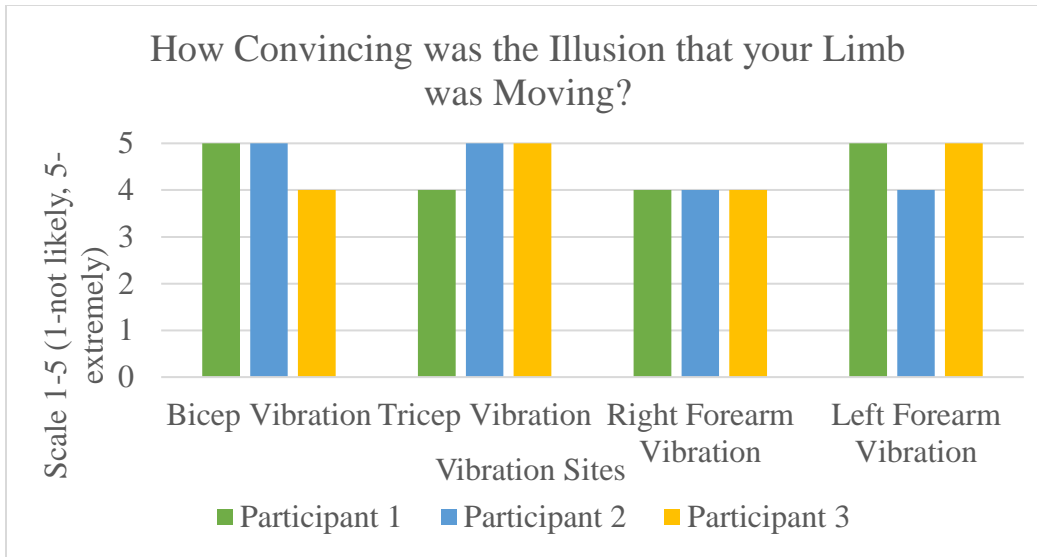


Figure 20: Strength of Illusion

The results of the range of motion quantified as the angular displacement as measured from their rested position to the final position of their limb are reported in Table 5 and illustrated in Figures 21-24.

Table 5: Range of Motion

Participant	Bicep	Triceps	Right Forearm	Left Forearm
1	50°	51°	4°	163°
2	131°	32°	45°	47°
3	54°	89°	15°	8°
Average	78.33°	57.33°	21.33°	72.66°

Across Participants 1-3, the bicep had an average range of motion at 78.33°, with the triceps quantified at 57.33°. The wrist supination and pronation were averaged at 21.33° and 72.66°, respectively.

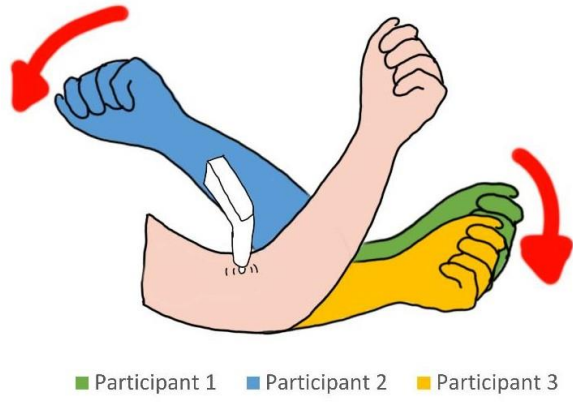


Figure 21: Range of Motion with Bicep Vibration

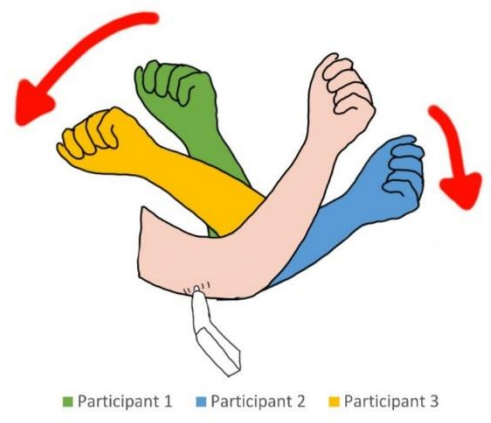


Figure 22: Range of Motion with Triceps Vibration

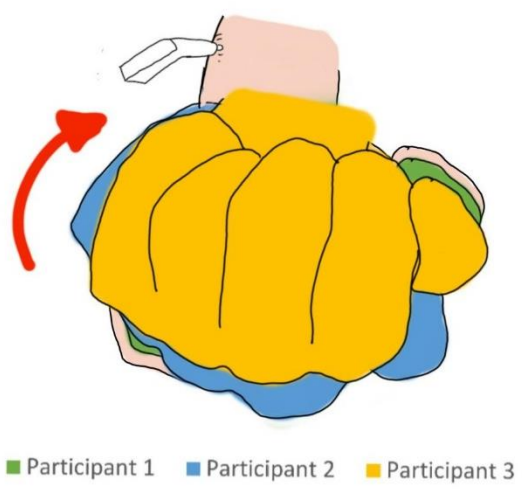
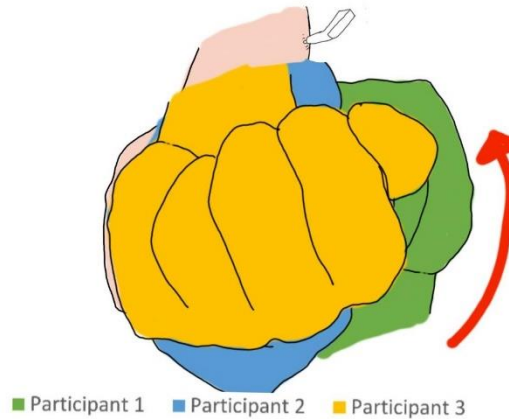


Figure 23: Range of Motion with Right Forearm Vibration



*Figure 24: Range of Motion with Left Forearm Vibration*

The velocities for Participants 1-3's strongest sensation of movement are presented in Table

6.

*Table 6: Velocity of Motions*

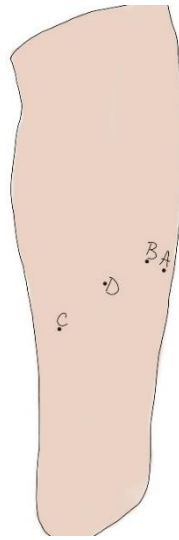
	Participant	1	2	3	Average
Bicep	Time to Move (s)	1.00	5.22	1.99	2.74
	Velocity (ROM/Time to Move)	50.20	25.10	27.16	34.15
Triceps	Time to Move (s)	5.95	3.99	10.36	6.77
	Velocity (ROM/Time to Move)	8.57	8.02	8.59	8.40
Right Forearm	Time to Move (s)	1.34	1.96	4.20	2.51
	Velocity (ROM/Time to Move)	2.99	22.79	3.57	9.78
Left Forearm	Time to Move (s)	0.99	0.50	0.34	0.61
	Velocity (ROM/Time to Move)	165.31	94.00	23.53	94.28

The average velocity for Participants 1-3 for the bicep and triceps were 34.15 °/s and 8.40 °/s, respectively. The average velocity for their wrist supination and pronation averaged at 9.78 °/s and 94.28 °/s, respectively.

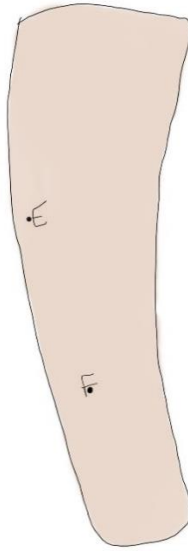
#### 4.2.3.B N-TMR

When testing with the N-TMR participant, the goal was to determine if it was possible to elicit the Kinesthetic Illusion. This would provide information on how well the device works and that the Kinesthetic Illusion works with N-TMR surgeries. The data presented are the vibration location and the sensations elicited.

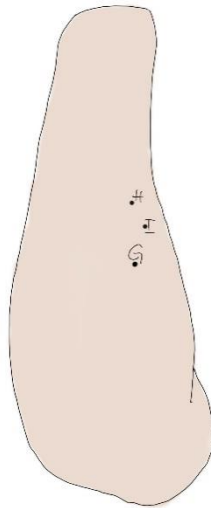
Figures 25-27 show the labeled vibration sites around the forearm.



*Figure 25: Ventral Forearm Vibration Sites*



*Figure 26: Lateral Forearm Vibration Site*





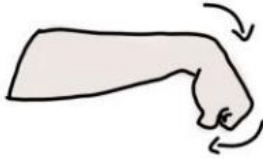


*Figure 27: Dorsal of Forearm Vibration Site*


Table 7 shows the movement sensations elicited at each site, with multiple sites eliciting similar sensations. Nine sites elicited a sensation of motion (A-E) with the described sensation illustrated next to each site. The participant reported a reset type of movement sensation at each site, where the sensation of his missing limb would revert to his resting position once the vibration stimulation was removed. The participant reported the convincingness of the illusion



between 2 (barely) to 4 (very), with an average of 3.5 (somewhat-very). This value indicates that there was a level of convincingness in the Kinesthetic Illusion for a person with N-TMR surgery.

Table 7: Sensations Elicited

Site	Sensation	Type of Movement	Strength of Illusion
A, D, G, I	Fist 	Sensation of motion stopped at a certain position. When the vibration stopped, the sensation reverted to resting position.	2
F	Fingers 3-5 Close 	Sensation of motion stopped at a certain position. When the vibration stopped, the sensation reverted to resting position.	3
H	Wrist Flexion with Fingers Closing 	Sensation of motion stopped at a certain position. When the vibration stopped, the sensation reverted to resting position.	2-3
B	Pinch 	Sensation of motion stopped at a certain position. When the vibration stopped, the sensation reverted to resting position.	3-4
C	Thumb Extension 	Sensation of motion stopped at a certain position. When the vibration stopped, the sensation reverted to resting position.	2

E	<p style="text-align: center;">Thumb Flexion</p> 	<p>Sensation of motion stopped at a certain position. When the vibration stopped, the sensation reverted to resting position.</p>	2
---	--	---	---

### 4.3 Discussion

#### 4.3.A Able-Bodied

Able-bodied participants were tested first to examine how well the device was able to induce its intended function of eliciting the Kinesthetic Illusion. The illusion was characterized by the time it took to first feel the Kinesthetic Illusion, the convincingness of the illusion, the range of motion, and the velocity of motion [58], [66], [90]. While various studies have used these values to characterize the illusion, the physical locations of stimulation on each muscle group are seldom reported to the degree of specificity we present here, and the movement characteristics are often not quantitatively captured [90]. Thus, it was challenging to compare the quantitative values found in this work directly to others. Although the quantitative values of our results cannot be directly compared to previous literature, the sensations and descriptions of the Kinesthetic Illusion reported by our participants can be compared. Below we discuss how our work compares to others.

The tonic vibration reflex is a separate phenomenon from the kinesthetic illusion and described as a muscle contraction due to vibration [91]. It is an involuntary phenomenon which can be visibly seen by a twitch or contraction of the vibrated muscle group [91], [92]. To ensure that the sensations our cohort was reporting at the vibration sites were not tonic vibration reflex and rather a movement illusion, we were constantly monitoring the vibrated muscle to look for signs of twitching and involuntary movement. If the participant presented muscle activity or

reported muscle contraction sensations consistent with the tonic vibration, we removed the HummingBear and had the participants rest and relax their muscles. Once the participants were relaxed, we continued the experiment. When the participants reported sensations that were not simply vibration (e.g., movement, tingling, cramping), we made sure the muscle area being vibrated was relaxed and no signs of toxic vibration reflex were observed.

Multisensory integration illusions are possible when other sensory modalities are combined with the Kinesthetic Illusion. One such illusion is the Pinocchio Illusion [55]–[57]. The Pinocchio Illusion entails a person pinching their nose with their eyes closed. When vibrating their biceps in this position, the participant will feel their elbow extending while their hand remains in contact with the nose. This conflicting sensory information is commonly perceived as the arm is pulling the nose away from the face, thus growing the length of the nose like Pinocchio. The external objects or other body parts in contact with the vibrated limb may stimulate cutaneous channels in the vibrated limb and can produce similar conflicting multi-sensory information. Participants 1-3 all reported sensations of the box their arm was rested on “engulfing” their arm and moving with their arm as if it were being pushed by their stimulated limb. These cutaneous sensations coupled with movement sensation are very much in line with the Pinocchio illusion and further evidence that our participants were in fact experiencing the Kinesthetic Illusion.

Although the experiment was tested with five individuals, Participant 4 reported no sensations of motion. This is not unusual as a study with 15 participants reported five individuals unable to feel the Kinesthetic Illusion [58]. In our work, four participants described feeling a sensation of motion, with three participants reporting sensations that related to conventionally reported motions of the Kinesthetic Illusion. Participant 2 felt flexion in the bicep and extension in the triceps as noted in Figure 17 and 18, a sensation that is in the opposite direction of what is

conventional. Participant 2's description of movement sensations is not uncommon with many studies suggesting a portion of the population may experience movement sensations in reverse [58], [90], [93]. Participant 5 experienced consistent isolated finger motions with bicep and triceps vibration as opposed to the conventional forearm extension and flexion that would be anticipated. Although Participant 5 did not report the conventional sensations of upper limb vibrations, their reported sensations were consistent with the same muscle groups and stimulus locations eliciting the same sensations each time they were stimulated.

Examining how well the HummingBear can elicit the intended sensations of the Kinesthetic Illusion with a control group can establish the device as a working research tool. From confirming the effectiveness of the device, it can then be tested on varying unique individuals to test the strengths and translation of the Kinesthetic Illusion.

#### *4.3.B N-TMR*

Testing the HummingBear with an N-TMR participant elicited the Kinesthetic Illusion. The vibration sites for the N-TMR participant were focused on the residual limb to determine if the reinnervated areas could elicit specific sensations of motion in the missing hand. Eliciting the Kinesthetic Illusion with N-TMR individuals has not been previously reported. In fact, it has mainly been documented with able-bodied individuals and a very select few individuals who have undergone conventional prosthetic focused TMR and targeted sensory reinnervation [27]. By testing with our N-TMR participant, we were able to demonstrate that vibrating sites which have been reinnervated for pain prevention can in fact provide kinesthetic sensory feedback to the user. The N-TMR participant felt full finger motions (fist and wrist flexion) as well as individualized digit movement (thumb flexion and extension, pinch, and three finger flexion). Similar digit motions have been perceived by six individuals who have undergone conventional prosthetic

focused TMR [27]. These data suggest that the more common and less surgically complex N-TMR may offer possibilities for intuitive prosthetic sensory feedback experienced as movement in the user's missing limb. Thus, making advanced control systems more accessible for growing populations of amputees receiving N-TMR surgery, and further advancing control systems for mechatronic prostheses.

#### *4.3.C Future Directions*

Taken together the able-bodied and N-TMR testing provided evidence that the HummingBear can consistently elicit the kinesthetic illusion with similar perceptual properties to that which is described in research literature. This supports that the HummingBear is a capable research tool that can elicit the Kinesthetic Illusion in able-body and N-TMR cohorts. Future directions are to continue testing the device with a larger participant pool of able-bodied individuals and N-TMR amputees, as well as studying the effects and learning time of long-term vibration applications. By establishing this device for the study of the kinesthetic illusion, we can implement vibrations as a sensory feedback technique with prosthetic control methods. Thus, getting us one step closer to “closing the loop” for prosthetic control.

# Chapter 5: Conclusion

## 5.1 Summary

With many individuals with traumatic amputations now receiving N-TMR for neuroma and pain prevention, new opportunities are presenting to make advanced prostheses more accessible. In this work, the accuracy of sonomyography (SMG) techniques to predict missing hand motor intentions and the possibility of integrating the Kinesthetic Illusion techniques as a sensory feedback method were investigated to establish the feasibility of N-TMR for bionic control.

The integration of SMG and machine learning for prosthetic control with N-TMR participants can establish a motor control system that can predict intended motions. A control system with SMG can have fewer technical limitations, limitations that must be considered with current conventional surface-based control systems. Thus, this can help establish control systems that leverage N-TMR to detect minute activity in deep-seated muscle in the residuum for naturalistic and intuitive prosthetic operation.

To integrate sensory feedback for prosthetic control, an accessible research device needed to be designed. Due to the inaccessibility of vibration devices and the lack of direct control of the amplitude and frequency with current devices, the HummingBear was developed to help study the Kinesthetic Illusion and we plan for to open-source the device to improve the accessibility of sensory feedback devices.

Using the HummingBear to elicit the Kinesthetic Illusion, sensations of motion were found for able-bodied individuals and an individual with N-TMR. Working with able-bodied individuals tested the feasibility of the HummingBear to elicit the intended sensations. Testing the device with an individual with N-TMR and eliciting movement sensations demonstrated the feasibility for kinesthetic sensory feedback for individuals with N-TMR. Thus, establishing advanced integrated

limbs with motor control and sensory feedback as a possibility for this increasing population of individuals with traumatic amputations.

Despite the limited size of participant cohorts, the experimental protocols and the HummingBear demonstrated its feasibility in improving bionic control with prostheses for individuals with N-TMR amputations and establishing N-TMR for prosthetic control in addition to pain management. With a new control method and a new vibration research device, we are one step closer to “closing the loop” and creating an accessible integrated limb.

## **5.2 Future Directions**

To further improve and strengthen the findings in this work, a larger participant pool with N-TMR participants will be necessary for both SMG and vibration protocols. Other future directions will be to test the Kinesthetic Illusion concurrently with EMG and SMG to “close the loop” and to integrate the HummingBear with a prosthesis socket to begin testing N-TMR with an advanced integrated, mechatronic limb.

## REFERENCES

- [1] A. M. R. Agur and M. J. Lee, *Grant's Atlas of Anatomy*, 10th ed. Philadelphia, Pa: Lippincott Williams and Wilkins, 1999.
- [2] V. M. Zatsiorsky and M. L. Latash, "Prehension synergies," 2004. [Online]. Available: [www.acsm-essr.org](http://www.acsm-essr.org)
- [3] J. C. Tuthill and E. Azim, "Proprioception," *Current Biology*, vol. 28, no. 5, pp. R194–R203, Mar. 2018, doi: 10.1016/J.CUB.2018.01.064.
- [4] D. J. Magee, J. E. Zachazewski, and W. S. Quillen, *Pathology and Intervention in Musculoskeletal Rehabilitation*. Elsevier Health Sciences, 2008.
- [5] J. T. Belter, J. L. Segil, A. M. Dollar, and R. F. Weir, "Mechanical design and performance specifications of anthropomorphic prosthetic hands: A review," *J Rehabil Res Dev*, vol. 50, no. 5, pp. 599–618, 2013, doi: 10.1682/JRRD.2011.10.0188.
- [6] U. Wijk and I. Carlsson, "Forearm amputees' views of prosthesis use and sensory feedback," *Journal of Hand Therapy*, vol. 28, no. 3, pp. 269–278, Jul. 2015, doi: 10.1016/j.jht.2015.01.013.
- [7] U. Wijk, I. K. Carlsson, C. Antfolk, A. Björkman, and B. Rosén, "Sensory Feedback in Hand Prostheses: A Prospective Study of Everyday Use," *Front Neurosci*, vol. 14, Jul. 2020, doi: 10.3389/fnins.2020.00663.
- [8] J. S. Hebert *et al.*, "Quantitative Eye Gaze and Movement Differences in Visuomotor Adaptations to Varying Task Demands Among Upper-Extremity Prosthesis Users," *JAMA Netw Open*, vol. 2, no. 9, p. e1911197, Sep. 2019, doi: 10.1001/jamanetworkopen.2019.11197.



- [9] A. Akhtar, J. Cornman, J. Austin, and D. Bala, “TOUCH FEEDBACK AND CONTACT REFLEXES USING THE PSYONIC ABILITY HAND.”
- [10] L. J. Hargrove, B. A. Lock, and A. M. Simon, “Pattern recognition control outperforms conventional myoelectric control in upper limb patients with targeted muscle reinnervation,” in *Proceedings of the Annual International Conference of the IEEE Engineering in Medicine and Biology Society, EMBS*, 2013, pp. 1599–1602. doi: 10.1109/EMBC.2013.6609821.
- [11] A. D. Roche, H. Rehbaum, D. Farina, and O. C. Aszmann, “Prosthetic Myoelectric Control Strategies: A Clinical Perspective,” *Curr Surg Rep*, vol. 2, no. 3, Mar. 2014, doi: 10.1007/s40137-013-0044-8.
- [12] M. Abdoli-Eramaki, C. Damecour, J. Christenson, and J. Stevenson, “The effect of perspiration on the sEMG amplitude and power spectrum,” *Journal of Electromyography and Kinesiology*, vol. 22, no. 6, pp. 908–913, Dec. 2012, doi: 10.1016/J.JELEKIN.2012.04.009.
- [13] L. Hargrove, K. Englehart, and B. Hudgins, “The effect of electrode displacements on pattern recognition based myoelectric control,” in *2006 International Conference of the IEEE Engineering in Medicine and Biology Society*, 2006, pp. 2203–2206. doi: 10.1109/IEMBS.2006.260681.
- [14] I. Kyranou, S. Vijayakumar, and M. S. Erden, “Causes of performance degradation in non-invasive electromyographic pattern recognition in upper limb prostheses,” *Front Neurobot*, vol. 12, no. September, Sep. 2018, doi: 10.3389/fnbot.2018.00058.

- [15] E. Biddiss and T. Chau, "Upper limb prosthesis use and abandonment: A survey of the last 25 years," *Prosthetics and Orthotics International*, vol. 31, no. 3. pp. 236–257, Sep. 2007. doi: 10.1080/03093640600994581.
- [16] B. R. Peters, S. A. Russo, J. M. West, A. M. Moore, and S. A. Schulz, "Targeted muscle reinnervation for the management of pain in the setting of major limb amputation," *SAGE Open Med*, vol. 8, p. 205031212095918, Jan. 2020, doi: 10.1177/2050312120959180.
- [17] M. S. Gart, J. M. Souza, and G. A. Dumanian, "Targeted Muscle Reinnervation in the Upper Extremity Amputee: A Technical Roadmap," *Journal of Hand Surgery*, vol. 40, no. 9. W.B. Saunders, pp. 1877–1888, Sep. 01, 2015. doi: 10.1016/j.jhsa.2015.06.119.
- [18] T. A. Kuiken, A. E. Schultz. Feuser, and A. K. Barlow, *Targeted muscle reinnervation : a neural interface for artificial limbs*. in Series in medical physics and biomedical engineering ; 28. Boca Raton: CRC Press, 2013. doi: 10.1201/b15079.
- [19] T. A. Kuiken\*\*, G. A. Dumanian, R. D. Lipschutz, L. A. Miller, and K. A. Stubblefield, "The use of targeted muscle reinnervation for improved myoelectric prosthesis control in a bilateral shoulder disarticulation amputee," 2004.
- [20] T. A. Kuiken, L. A. Miller, K. Turner, and L. J. Hargrove, "A Comparison of Pattern Recognition Control and Direct Control of a Multiple Degree-of-Freedom Transradial Prosthesis," *IEEE J Transl Eng Health Med*, vol. 4, 2016, doi: 10.1109/JTEHM.2016.2616123.
- [21] T. A. Kuiken *et al.*, "Targeted muscle reinnervation for real-time myoelectric control of multifunction artificial arms," *JAMA*, vol. 301, no. 6, pp. 619–628, Feb. 2009, doi: 10.1001/jama.2009.116.

- [22] L. J. Hargrove, L. A. Miller, K. Turner, and T. A. Kuiken, “Myoelectric Pattern Recognition Outperforms Direct Control for Transhumeral Amputees with Targeted Muscle Reinnervation: A Randomized Clinical Trial,” *Sci Rep*, vol. 7, no. 1, Dec. 2017, doi: 10.1038/s41598-017-14386-w.
- [23] D. C. Tkach, A. J. Young, L. H. Smith, E. J. Rouse, and L. J. Hargrove, “Real-time and offline performance of pattern recognition myoelectric control using a generic electrode grid with targeted muscle reinnervation patients,” *IEEE Transactions on Neural Systems and Rehabilitation Engineering*, vol. 22, no. 4, pp. 727–734, 2014, doi: 10.1109/TNSRE.2014.2302799.
- [24] T. A. Kuiken *et al.*, “Targeted muscle reinnervation for real-time myoelectric control of multifunction artificial arms,” *JAMA*, vol. 301, no. 6, pp. 619–628, Feb. 2009, doi: 10.1001/jama.2009.116.
- [25] T. A. Kuiken, A. K. Barlow, L. J. Hargrove, and G. A. Dumanian, “Targeted muscle reinnervation for the upper and lower extremity,” *Techniques in Orthopaedics*, vol. 32, no. 2, pp. 109–116, 2017, doi: 10.1097/BTO.000000000000194.
- [26] T. A. Kuiken, L. A. Miller, K. Turner, and L. J. Hargrove, “A Comparison of Pattern Recognition Control and Direct Control of a Multiple Degree-of-Freedom Transradial Prosthesis,” *IEEE J Transl Eng Health Med*, vol. 4, 2016, doi: 10.1109/JTEHM.2016.2616123.
- [27] P. D. Marasco *et al.*, “Illusory movement perception improves motor control for prosthetic hands,” 2018. [Online]. Available: <https://www.science.org>

- [28] T. A. Kuiken *et al.*, “Redirection of cutaneous sensation from the hand to the chest skin of human amputees with targeted reinnervation,” 2007. [Online]. Available: [www.pnas.org/cgi/doi/10.1073/pnas.0706525104](http://www.pnas.org/cgi/doi/10.1073/pnas.0706525104)
- [29] J. W. Sensinger, A. E. Schultz, and T. A. Kuiken, “Examination of force discrimination in human upper limb amputees with reinnervated limb sensation following peripheral nerve transfer,” *IEEE Transactions on Neural Systems and Rehabilitation Engineering*, vol. 17, no. 5, pp. 438–444, Oct. 2009, doi: 10.1109/TNSRE.2009.2032640.
- [30] A. E. Schultz, P. D. Marasco, and T. A. Kuiken, “Vibrotactile detection thresholds for chest skin of amputees following targeted reinnervation surgery,” *Brain Res*, vol. 1251, pp. 121–129, Jan. 2009, doi: 10.1016/j.brainres.2008.11.039.
- [31] J. S. Hebert, K. M. Chan, and M. R. Dawson, “Cutaneous sensory outcomes from three transhumeral targeted reinnervation cases,” *Prosthet Orthot Int*, vol. 40, no. 3, pp. 303–310, Jun. 2016, doi: 10.1177/0309364616633919.
- [32] F. Kaneko, E. Shibata, T. Hayami, K. Nagahata, and T. Aoyama, “The association of motor imagery and kinesthetic illusion prolongs the effect of transcranial direct current stimulation on corticospinal tract excitability,” *J Neuroeng Rehabil*, vol. 13, no. 1, Apr. 2016, doi: 10.1186/s12984-016-0143-8.
- [33] I. Bufalari, A. Sforza, P. Cesari, S. M. Aglioti, and A. D. Fourkas, “Motor imagery beyond the joint limits: A transcranial magnetic stimulation study,” *Biol Psychol*, vol. 85, no. 2, pp. 283–290, Oct. 2010, doi: 10.1016/j.biopsycho.2010.07.015.
- [34] J. S. Hebert *et al.*, “Novel targeted sensory reinnervation technique to restore functional hand sensation after transhumeral amputation,” *IEEE Transactions on Neural Systems and*

- Rehabilitation Engineering*, vol. 22, no. 4, pp. 765–773, 2014, doi: 10.1109/TNSRE.2013.2294907.
- [35] J. S. Schofield, C. E. Shell, D. T. Beckler, Z. C. Thumser, and P. D. Marasco, “Long-Term Home-Use of Sensory-Motor-Integrated Bidirectional Bionic Prosthetic Arms Promotes Functional, Perceptual, and Cognitive Changes,” *Front Neurosci*, vol. 14, Feb. 2020, doi: 10.3389/fnins.2020.00120.
- [36] L. M. Mioton *et al.*, “Targeted Muscle Reinnervation Improves Residual Limb Pain, Phantom Limb Pain, and Limb Function: A Prospective Study of 33 Major Limb Amputees,” *Clin Orthop Relat Res*, vol. 478, no. 9, pp. 2161–2167, Sep. 2020, doi: 10.1097/CORR.0000000000001323.
- [37] A. G. Chappell, S. W. Jordan, and G. A. Dumanian, “Targeted Muscle Reinnervation for Treatment of Neuropathic Pain,” *Clinics in Plastic Surgery*, vol. 47, no. 2. W.B. Saunders, pp. 285–293, Apr. 01, 2020. doi: 10.1016/j.cps.2020.01.002.
- [38] J. M. Souza, J. E. Cheesborough, J. H. Ko, M. S. Cho, T. A. Kuiken, and G. A. Dumanian, “Targeted Muscle Reinnervation: A Novel Approach to Postamputation Neuroma Pain,” *Clin Orthop Relat Res*, vol. 472, no. 10, pp. 2984–2990, Oct. 2014, doi: 10.1007/s11999-014-3528-7.
- [39] B. R. Peters, S. A. Russo, J. M. West, A. M. Moore, and S. A. Schulz, “Targeted muscle reinnervation for the management of pain in the setting of major limb amputation,” *SAGE Open Med*, vol. 8, p. 205031212095918, Jan. 2020, doi: 10.1177/2050312120959180.
- [40] S. Salminger *et al.*, “Current rates of prosthetic usage in upper-limb amputees—have innovations had an impact on device acceptance?,” *Disabil Rehabil*, vol. 44, no. 14, pp. 3708–3713, 2022, doi: 10.1080/09638288.2020.1866684.

- [41] K. Ziegler-Graham, E. J. MacKenzie, P. L. Ephraim, T. G. Travison, and R. Brookmeyer, “Estimating the Prevalence of Limb Loss in the United States: 2005 to 2050,” *Arch Phys Med Rehabil*, vol. 89, no. 3, pp. 422–429, Mar. 2008, doi: 10.1016/j.apmr.2007.11.005.
- [42] J. M. Souza, J. E. Cheesborough, J. H. Ko, M. S. Cho, T. A. Kuiken, and G. A. Dumanian, “Targeted Muscle Reinnervation: A Novel Approach to Postamputation Neuroma Pain,” *Clin Orthop Relat Res*, vol. 472, no. 10, pp. 2984–2990, Oct. 2014, doi: 10.1007/s11999-014-3528-7.
- [43] A. S. Dhawan *et al.*, “Proprioceptive Sonomyographic Control: A novel method for intuitive and proportional control of multiple degrees-of-freedom for individuals with upper extremity limb loss,” *Sci Rep*, vol. 9, no. 1, Dec. 2019, doi: 10.1038/s41598-019-45459-7.
- [44] V. Nazari and Y. P. Zheng, “Controlling Upper Limb Prostheses Using Sonomyography (SMG): A Review,” *Sensors*, vol. 23, no. 4. MDPI, Feb. 01, 2023. doi: 10.3390/s23041885.
- [45] S. Patwardhan, J. Schofield, W. M. Joiner, and S. Sikdar, “Sonomyography shows feasibility as a tool to quantify joint movement at the muscle level,” in *IEEE International Conference on Rehabilitation Robotics*, IEEE Computer Society, 2022. doi: 10.1109/ICORR55369.2022.9896582.
- [46] X. Chen, Y. P. Zheng, J. Y. Guo, and J. Shi, “Sonomyography (smg) control for powered prosthetic hand: A Study with normal subjects,” *Ultrasound Med Biol*, vol. 36, no. 7, pp. 1076–1088, 2010, doi: 10.1016/j.ultrasmedbio.2010.04.015.
- [47] J. Shi, Q. Chang, and Y. P. Zheng, “Feasibility of controlling prosthetic hand using sonomyography signal in real time: Preliminary study,” *J Rehabil Res Dev*, vol. 47, no. 2, pp. 87–98, 2010, doi: 10.1682/JRRD.2009.03.0031.

- [48] V. Nazari and Y.-P. Zheng, “Controlling Upper Limb Prostheses Using Sonomyography (SMG): A Review,” *Sensors*, vol. 23, no. 4, p. 1885, Feb. 2023, doi: 10.3390/s23041885.
- [49] J. Shi, Q. Chang, and Y. P. Zheng, “Feasibility of controlling prosthetic hand using sonomyography signal in real time: Preliminary study,” *J Rehabil Res Dev*, vol. 47, no. 2, pp. 87–98, 2010, doi: 10.1682/JRRD.2009.03.0031.
- [50] A. S. Dhawan *et al.*, “Proprioceptive Sonomyographic Control: A novel method for intuitive and proportional control of multiple degrees-of-freedom for individuals with upper extremity limb loss,” *Sci Rep*, vol. 9, no. 1, Dec. 2019, doi: 10.1038/s41598-019-45459-7.
- [51] Y. Fang, N. Hettiarachchi, D. Zhou, and H. Liu, “Multi-modal sensing techniques for interfacing hand prostheses: A review,” *IEEE Sens J*, vol. 15, no. 11, pp. 6065–6076, Nov. 2015, doi: 10.1109/JSEN.2015.2450211.
- [52] V. Nazari and Y.-P. Zheng, “Controlling Upper Limb Prostheses Using Sonomyography (SMG): A Review,” *Sensors*, vol. 23, no. 4, p. 1885, Feb. 2023, doi: 10.3390/s23041885.
- [53] X. Chen, Y. P. Zheng, J. Y. Guo, and J. Shi, “Sonomyography (smg) control for powered prosthetic hand: A Study with normal subjects,” *Ultrasound Med Biol*, vol. 36, no. 7, pp. 1076–1088, 2010, doi: 10.1016/j.ultrasmedbio.2010.04.015.
- [54] G. M. Goodwin, D. I. McCloskey, and P. B. C. Matthews, “Proprioceptive Illusions Induced by Muscle Vibration: Contribution by Muscle Spindles to Perception?,” 1972.
- [55] C. C. Berger, B. Lin, B. Lenggenhager, J. Lanier, and M. Gonzalez-Franco, “Follow Your Nose: Extended Arm Reach After Pinocchio Illusion in Virtual Reality,” *Front Virtual Real*, vol. 3, May 2022, doi: 10.3389/frvir.2022.712375.

- [56] J. R. Purcell, J. Chen, A. B. Moussa-Tooks, and W. P. Hetrick, “Psychometric evaluation of the Pinocchio Illusion Questionnaire,” *Atten Percept Psychophys*, vol. 82, no. 5, pp. 2728–2737, Jul. 2020, doi: 10.3758/s13414-020-02011-4.
- [57] A. Burrack and P. Brugger, “Individual differences in susceptibility to experimentally induced phantom sensations,” *Body Image*, vol. 2, no. 3, pp. 307–313, Sep. 2005, doi: 10.1016/j.bodyim.2005.04.002.
- [58] J. S. Schofield, M. R. Dawson, J. P. Carey, and J. S. Hebert, “Characterizing the effects of amplitude, frequency and limb position on vibration induced movement illusions: Implications in sensory-motor rehabilitation,” *Technology and Health Care*, vol. 23, no. 2, pp. 129–141, 2015, doi: 10.3233/THC-140879.
- [59] G. M. Goodwin, D. I. McCloskey, and P. B. C. Matthews, “THE CONTRIBUTION OF MUSCLE AFFERENTS TO KESLESTHESIA SHOWN BY VIBRATION INDUCED ILLUSIONS OF MOVEMENT AND BY THE EFFECTS OF PARALYSING JOINT AFFERENTS,” 1972. [Online]. Available: <https://academic.oup.com/brain/article/95/4/705/350578>
- [60] S. G. Meek, S. C. Jacobsen, and P. P. Goulding, “Department Veterans Affairs Extended physiologic taction : Design and evaluation of a proportional force feedback system.”
- [61] G. Eklund, “Position sense and state of contraction; the effects of vibration,” 1972.
- [62] L. A. Jones, “Motor Illusions: What Do They Reveal About Proprioception?,” 1988.
- [63] J. R. Lackner, “Human Sensory-Motor Adaptation to the Terrestrial Force Environment,” in *Brain Mechanisms and Spatial Vision*, Springer Netherlands, 1985, pp. 175–209. doi: 10.1007/978-94-009-5071-9\_8.



- [64] J. P. Roll and J. P. Vedel, “\_’ mental Bran Research Kinaesthetic Role of Muscle Afferents in Man, Studied by Tendon Vibration and Microneurography,” 1982.
- [65] T. Kito, T. Hashimoto, T. Yoneda, S. Katamoto, and E. Naito, “Sensory processing during kinesthetic aftereffect following illusory hand movement elicited by tendon vibration,” *Brain Res*, vol. 1114, no. 1, pp. 75–84, Oct. 2006, doi: 10.1016/j.brainres.2006.07.062.
- [66] S. Calvin-Figuere, P. Romaguere, and J.-P. Rolí Rolí, “Relations between the directions of vibration-induced kinesthetic illusions and the pattern of activation of antagonist muscles,” 2000. [Online]. Available: [www.elsevier.com/locate/bres](http://www.elsevier.com/locate/bres)
- [67] C. Capaday and J. D. Cooke, “The Effects of Muscle Vibration on the Attainment of Intended Final Position During Voluntary Human Arm Movements\*,” 1981.
- [68] S. M. P. Verschueren, S. Brumagne, S. P. Swinnen, and P. J. Cordo, “The effect of aging on dynamic position sense at the ankle.” [Online]. Available: [www.elsevier.com/locate/bbr](http://www.elsevier.com/locate/bbr)
- [69] J. P. Roll, J. P. Vedel, and E. Ribot, “Alteration of proprioceptive messages induced by tendon vibration in man: a microneurographic study,” 1989.
- [70] T. Seizova-Cajic, J. L. Smith, J. L. Taylor, and S. C. Gandevia, “Proprioceptive movement illusions due to prolonged stimulation: Reversals and aftereffects,” *PLoS One*, vol. 2, no. 10, Oct. 2007, doi: 10.1371/journal.pone.0001037.
- [71] O. White and U. Proske, “Illusions of forearm displacement during vibration of elbow muscles in humans,” *Exp Brain Res*, vol. 192, no. 1, pp. 113–120, Jan. 2009, doi: 10.1007/s00221-008-1561-z.
- [72] I. Bufalari, A. Sforza, P. Cesari, S. M. Aglioti, and A. D. Fourkas, “Motor imagery beyond the joint limits: A transcranial magnetic stimulation study,” *Biol Psychol*, vol. 85, no. 2, pp. 283–290, Oct. 2010, doi: 10.1016/j.biopsycho.2010.07.015.

- [73] F. Kaneko, E. Shibata, T. Hayami, K. Nagahata, and T. Aoyama, “The association of motor imagery and kinesthetic illusion prolongs the effect of transcranial direct current stimulation on corticospinal tract excitability,” *J Neuroeng Rehabil*, vol. 13, no. 1, Apr. 2016, doi: 10.1186/s12984-016-0143-8.
- [74] N. Kriegeskorte and R. A. Kievit, “Representational geometry: Integrating cognition, computation, and the brain,” *Trends in Cognitive Sciences*, vol. 17, no. 8. pp. 401–412, Aug. 2013. doi: 10.1016/j.tics.2013.06.007.
- [75] M. Atzori, H. Muller, and M. Baechler, “Recognition of hand movements in a trans-radial amputated subject by sEMG,” in *IEEE International Conference on Rehabilitation Robotics*, 2013. doi: 10.1109/ICORR.2013.6650486.
- [76] A. A. Adewuyi, L. J. Hargrove, and T. A. Kuiken, “An Analysis of Intrinsic and Extrinsic Hand Muscle EMG for Improved Pattern Recognition Control,” *IEEE Transactions on Neural Systems and Rehabilitation Engineering*, vol. 24, no. 4, pp. 485–494, Apr. 2016, doi: 10.1109/TNSRE.2015.2424371.
- [77] G. Li and T. A. Kuiken, “EMG pattern recognition control of multifunctional prostheses by transradial amputees,” in *Proceedings of the 31st Annual International Conference of the IEEE Engineering in Medicine and Biology Society: Engineering the Future of Biomedicine, EMBC 2009*, IEEE Computer Society, 2009, pp. 6914–6917. doi: 10.1109/IEMBS.2009.5333628.
- [78] V. K. Nanayakkara, G. Cotugno, N. Vitzilaios, D. Venetsanos, T. Nanayakkara, and M. N. Sahinkaya, “The Role of Morphology of the Thumb in Anthropomorphic Grasping: A Review,” *Frontiers in Mechanical Engineering*, vol. 3. Frontiers Media S.A., 2017. doi: 10.3389/fmech.2017.00005.

- [79] C. E. Lang, S. L. DeJong, and J. A. Beebe, "Recovery of thumb and finger extension and its relation to grasp performance after stroke," *J Neurophysiol*, vol. 102, no. 1, pp. 451–459, Jul. 2009, doi: 10.1152/jn.91310.2008.
- [80] L. Resnik *et al.*, "Advanced upper limb prosthetic devices: Implications for upper limb prosthetic rehabilitation," *Archives of Physical Medicine and Rehabilitation*, vol. 93, no. 4. W.B. Saunders, pp. 710–717, 2012. doi: 10.1016/j.apmr.2011.11.010.
- [81] F. Cordella *et al.*, "Literature review on needs of upper limb prosthesis users," *Frontiers in Neuroscience*, vol. 10, no. MAY. Frontiers Media S.A., 2016. doi: 10.3389/fnins.2016.00209.
- [82] L. V. Mcfarland, S. L. H. Winkler, A. W. Heinemann, M. Jones, and A. Esquenazi, "Unilateral upper-limb loss: Satisfaction and prosthetic-device use in veterans and servicemembers from Vietnam and OIF/OEF conflicts," *J Rehabil Res Dev*, vol. 47, no. 4, pp. 299–316, 2010, doi: 10.1682/JRRD.2009.03.0027.
- [83] B. Peerdeman *et al.*, "Myoelectric forearm prostheses: State of the art from a user-centered perspective," *The Journal of Rehabilitation Research and Development*, vol. 48, no. 6, p. 719, 2011, doi: 10.1682/JRRD.2010.08.0161.
- [84] "TECHNO CONCEPT."
- [85] S. M. P. Verschueren, P. J. Cordo, and S. P. Swinnen, "Representation of Wrist Joint Kinematics by the Ensemble of Muscle Spindles From Synergistic Muscles," 1998.
- [86] D. J. Goble and S. H. Brown, "The biological and behavioral basis of upper limb asymmetries in sensorimotor performance," *Neuroscience and Biobehavioral Reviews*, vol. 32, no. 3. pp. 598–610, 2008. doi: 10.1016/j.neubiorev.2007.10.006.

- [87] E. Tidoni, G. Fusco, D. Leonardis, A. Frisoli, M. Bergamasco, and S. M. Aglioti, “Illusory movements induced by tendon vibration in right- and left-handed people,” *Exp Brain Res*, vol. 233, no. 2, pp. 375–383, Feb. 2015, doi: 10.1007/s00221-014-4121-8.
- [88] N. Hagura *et al.*, “Activity in the posterior parietal cortex mediates visual dominance over kinesthesia,” *Journal of Neuroscience*, vol. 27, no. 26, pp. 7047–7053, Jun. 2007, doi: 10.1523/JNEUROSCI.0970-07.2007.
- [89] F. Ferrari *et al.*, “Proprioceptive Augmentation With Illusory Kinaesthetic Sensation in Stroke Patients Improves Movement Quality in an Active Upper Limb Reach-and-Point Task,” *Front Neurobot*, vol. 15, Mar. 2021, doi: 10.3389/fnbot.2021.610673.
- [90] F. Ferrari, F. Clemente, and C. Cipriani, “The preload force affects the perception threshold of muscle vibration-induced movement illusions,” *Exp Brain Res*, vol. 237, no. 1, pp. 111–120, Jan. 2019, doi: 10.1007/s00221-018-5402-4.
- [91] E. Kalaoğlu *et al.*, “High-frequency whole-body vibration activates tonic vibration reflex.,” *Turk J Phys Med Rehabil*, vol. 69, no. 1, pp. 46–51, Mar. 2023, doi: 10.5606/tftrd.2023.10854.
- [92] “Whole Body Vibration and Tonic Vibration Reex,” 2022. [Online]. Available: <https://beta.clinicaltrials.gov/study/NCT05209945>
- [93] M. W. Taylor, J. L. Taylor, and T. Seizova-Cajic, “Muscle Vibration-Induced Illusions: Review of Contributing Factors, Taxonomy of Illusions and User’s Guide,” *Multisensory Research*, vol. 30, no. 1. Brill Academic Publishers, pp. 25–63, 2017. doi: 10.1163/22134808-00002544.

# Appendix

## Appendix A: MATLAB Code and Function

*Movement Vibration Code:*

Vibration Tool %%

Anna Rita Moukarzel Vibrate motor at 20 Hz and 90 Hz and time run time

```
clear all
close all
clc
```

Subject File Set Up %%

```
SubjectFoldername = 'Numtest2'; %Change name of folder per participant
overallDataFilepath = 'C:\Users\armou\Desktop\Lab\Thesis\testing'; %sets direction to where
you want folder saved
cd(overallDataFilepath) %goes to that location in computer
mkdir(SubjectFoldername) %creates folder under name
cd(SubjectFoldername) %goes to that location in computer
mkdir('20') %makes folder for 20 Hz to save in
mkdir('90') %makes folder for 90 Hz to save in
```

Call Arduino and ESC %%

```
a = arduino('COM3','Nano3','Libraries','Servo'); %change COM3 to your computers USB port
s = servo(a,'D8'); %call motor as servo
```

Get User Input %%

```
%this is a loop to allow user to call and switch the vibrations from 20 Hz to 90 Hz
while true
    user_input = input("Please Type '20' or '90' for Frequency Level"); %prompt and user input
    u = cast(user_input,"uint8"); %saves input as integer
```

```

cd(overallDataFilepath) %goes back to main location where function on compute is
    if u == 20 %loop for if call 20 Hz
        Vibration_Function(SubjectFoldername,overallDataFilepath,u,s,0.31); % 0.31 found
position of motor to be 20 Hz, calls on files and variables for vibration function
    elseif u == 90 %loop for if call 90 Hz
        Vibration_Function(SubjectFoldername,overallDataFilepath,u,s,0.39); % 0.39 found
position of motor to be 90 Hz, calls on files and variables for vibration function
    else
        break
    end
end

```

Published with MATLAB® R2022a

*Vibration Function:*

Function Code for Vibration %%

```

%Anna Rita Moukarzel
function Vibration_Function(SubjectFoldername,overallDataFilepath,u,s,f) %variables used in
function, u=userinput of 20 or 90, s calls servo, f is set frequency number

```

Create Subject Files

```

cd(overallDataFilepath) %gets file path ready
cd(SubjectFoldername) %go to folder
hzfolder=int2str(u); %reads user frequency number input and turns into string
cd(hzfolder) %sends path inside the 20 or 90 folder

```

Camera Function %%

```

vidobj = videoinput('winvideo', 'c922 Pro Stream Webcam');
fps = 15; % frames per second
vidobj.FramesPerTrigger = Inf; % Configure the number of frames to log.

```

```

%Skip the first few frames the device provides before logging data.
vidobj.TriggerFrameDelay = 5;
    % Access the device's video source.
    src = getselectedsource(vidobj);
    % Check the device specific frame rates (frames per second) available.
    frameRates = set(src, 'FrameRate');
    % Configure the device's frame rate to the highest available setting.
    src.FrameRate = frameRates{4}; %30 frames per second
    actualRate = str2num( frameRates{4});
    % THE RECORD TIME

%frameRates{1='30.0000';2='24.0000';3='20.0000';4='15.0000';5='10.0000';6='7.5000';7='5.000
0'}

```

#### Vibration Function %%

```

    writePosition(s,0.25); %allows motor to receive some voltage but not enough to start (allows
for faster jumps)
    pause(.25)
    name_test = input("Please name Trial Number"); %prompt to enter trial number
    ready_prompt = strcat("Begin test ", num2str(name_test));
    ready_prompt = strcat(ready_prompt, ". Press Enter to start"); %prompt to begin test
    ready = input(ready_prompt); %prompt to begin motor

    start(vidobj) %starts camera
    writePosition(s,f); %runs motor at designated angle for 20 or 90 Hz
    fl = figure(); %this is to run CurrentCharacter
    time_table = []; %this is to store times
    u_input = '+'; %this is a chosen character that is difficult to press on a keyboard so a user does
not accidentally press
    tic %start timer
    disp("Press '0' to end trial")

```

```

%this loop mimics an infinite loop to keep motor running as long as needed
while(1)
    figure(f1) %this figure allows you to press any key while in the infinite loop
    u_input = f1.CurrentCharacter; %press any key
    if u_input == '0' %this ends the infinite loop
        time_table = [time_table; toc]
        vidobj.TimerFcn = {'stop'};
        break
    elseif u_input ~= '+' %you can press any key beside '+' to register time into table while loop
running
        time_table = [time_table; toc]
        f1.CurrentCharacter = '+';
        disp("Press '0' to end trial")
    end
    pause(.25)
end

writePosition(s,0.25); %stops motor, it is at 0.25 because this stops the motor but still allows it
to jump faster to each frequency
pause(.25)
clc

%camera save data
videoData = get(vidobj);
numFrames = videoData.FramesAcquired; % Acquired the number of frames
[frames, timeStamp,~] = getdata(vidobj,numFrames); % get data

% Acquires video data
vidWriter = VideoWriter(strcat(hzfolder, " - ",num2str(name_test),'.avi'));
vidWriter.FrameRate = fps;
open(vidWriter);

```



```

for i = 1:numel(timeStamp)
    img = frames(:,:,i); % get image
    writeVideo(vidWriter,img);% Write frame to video
end
close(vidWriter);
delete(vidobj)
clear vidobj
pause(.25)

```

```

% This section saves the data collected and moves onto another trial or Hz
tablename = strcat('Times ', num2str(name_test)); %saves table to test number
writematrix(time_table, num2str(name_test)); %save table to folder

```

Prompt to continue with trials under current Hz or change Hz

```

trial = strcat("Continue to Next Trial? press '1' to continue or '0' to end" ); %user input to
continue same Hz Trials
trial_continue = input(trial);
t_continue = cast(trial_continue,"uint8"); %convert double to integer
if t_continue == 1
    Vibration_Function(SubjectFoldername,overallDataFilepath,u,s,f); %this calls function to
start again for another trial
elseif t_continue == 0 %this takes back to code to switch frequencies
    ;
end

```

```

end

```

Published with MATLAB® R2022a